Science of the Total Environment 885 (2023) 163963

Contents lists available at ScienceDirect

Science of the Total Environment

journal homepage: www.elsevier.com/locate/scitotenv

Review

A review on LED technology in water photodisinfection

Miguel Martín-Sómer, Cristina Pablos, Cristina Adán, Rafael van Grieken, Javier Marugán *

Department of Chemical and Environmental Technology, ESCET, Universidad Rey Juan Carlos, C/ Tulipán s/n, 28933 Móstoles, Madrid, Spain

HIGHLIGHTS

- 265 nm wavelength have higher germicidal effect, but 280 nm represses cell repair.
- 280 nm LED have higher electricity-to-photon conversion compared to 265 nm LED.
- UVA exposure before UVC affects biological processes in bacterial inactivation.
- Pulsed UVC LED does not affect activity but improves temperature control.
- Expected deployment of UVC LED in the upcoming future in water disinfection

GRAPHICAL ABSTRACT

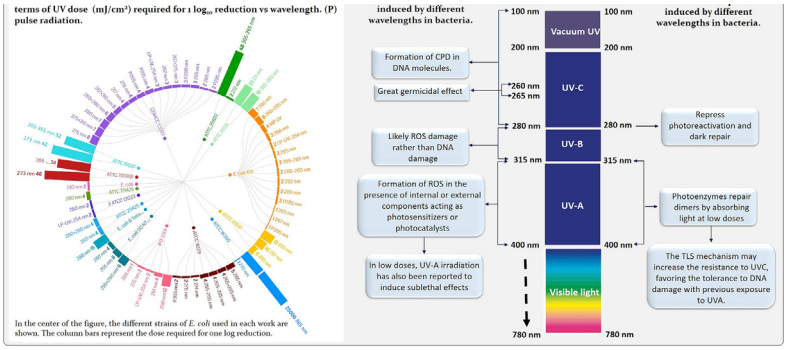

ARTICLE INFO

Editor: Damia Barcelo

Keywords:
Photoreactivation
Disinfection
Water treatment
Photodisinfection
UV LED

ABSTRACT

The increase in efficiency achieved by UV LED devices has led to a compelling increase in research reports on UV LED water treatment for consumption in the past few years. This paper presents an in-depth review based on recent studies on the suitability and performance of UV LED-driven processes for water disinfection. The effect of different UV wavelengths and their combinations was analysed for the inactivation of various microorganisms and the inhibition of repair mechanisms. Whereas 265 nm UVC LED present a higher DNA damaging potential, 280 nm radiation is reported to repress photoreactivation and dark repair. No synergistic effects have been proved to exist when coupling UVB + UVC whereas sequential UVA-UVC radiation seemed to enhance inactivation. Benefits of pulsed over continuous radiation in terms of germicidal effects and energy consumption were also analysed, but with inconclusive results. However, pulsed radiation may be promising for improving thermal management. As a challenge, the use of UV LED sources introduces significant inhomogeneities in the light distribution, pushing for the development of adequate simulation methods to ensure that the minimum target dose required for the target microbes is achieved. Concerning energy consumption, selecting the optimal wavelength of the UV LED needs a compromise between the quantum efficiency of the process and the electricity-to-photon conversion. The expected development of the UV LED industry in the next few years points to UVC LED as a promising technology for water disinfection at a large scale that could be competitive in the market in the near future.

Abbreviations: ARB, antibiotic-resistant bacteria; ARG, antibiotic-resistant gens; CPC, cyclobutane pyrimidine dimers; $E_{E,O}$, electrical consumption per order; FCV, Feline calcivirus; HAdV2, adenovirus serotype 2; HAdV5, adenovirus serotype 5; Hg-FL, mercury fluorescent lamp; IAVs, Influenza A viruses; LED, light-emitting diode; LP, low-pressure; MP, medium-pressure; ROS, reactive oxygen species; TLS, translation synthesis; TRB, tetracycline-resistant bacteria; WPE, wall plug efficiency.

* Corresponding author.
E-mail address: javier.marugan@urjc.es (J. Marugán).

http://dx.doi.org/10.1016/j.scitotenv.2023.163963
Received 22 February 2023; Received in revised form 19 April 2023; Accepted 1 May 2023
Available online 4 May 2023

Contents

1. Introduction

LED technology has opened up new opportunities for water disinfection through its high efficiency, long lifespan, and flexibility in wavelength selection. Compared to traditional lamps, UV LED are smaller, have no warm-up time, and can be precisely controlled for optimal disinfection. The availability of specific wavelengths also allows for targeted or combined multi-wavelength sources for treating multiple microbial targets. However, the use of LED lamps requires a precise understanding of photochemistry, reactor design, and the mechanism of microbial inactivation to optimise their performance. As the industry continues to develop more efficient UV LED technology, it is expected that UV LED systems will become a competitive option for large-scale water disinfection in the near future.

1.1. Development of LED and UV LED technologies

The development of the light-emitting diode (LED) started in 1907, with Henry Joseph Round, a British electrical engineer, who reported current-driven light emission using a polycrystalline material from silicon carbide (SiC), known as electroluminescence (Round, 1991). In the following years, this same phenomenon was observed in different crystalline materials, such as Ge, Si, carborundum, and copper oxide (Dupuis and Krames, 2008). In the 1940s, the existence within a crystalline SiC material of n-type regions dominated by negative charge carriers and p-type regions dominated by positively charged carriers was first described (Ohl, 1946). In the following decade, this phenomenon was also observed in other semiconductors that were capable of emitting light at other wavelengths (Rediker, 1987). The discovery of the p-n junction was a fundamental event for the development of the LED lighting systems that we know today. LED devices are systems capable of emitting light by electroluminescence when an electrical current is passed through them. This phenomenon only happens in one way, and the emission of light, unlike incandescent lamps, is not due to heating, but it is due to the selective jumping of electrons from the n-type to the p-type region. The energy released in this process and, therefore, the wavelength of the light emitted depend on the energy difference between the two regions and, therefore, on the semiconductor material used. One of the main characteristics of electroluminescence is that radiation is emitted in a very small range of wavelengths, which makes it possible to optimise the selection of LED for a specific application. Furthermore, it is important to note that one of the main advantages of LED is that almost all the energy released by the leap of electrons is transformed into light, so the efficiency of the process is very high (Weisbuch, 2020).

Although, the emission of light by semiconductors was discovered in the early 20th century, a practical version of visible (red) light was not developed until the early 1960s (Zheludev, 2007). These early devices could emit very low powers and were used only as indicators. Throughout the 1970s, the development of LED devices continued, and new devices with shorter wavelengths, such as orange, yellow, and green, were launched on the market. It was not until 1993 that a blue emitting LED was first developed (Lamar, 2020). In 1996, the first white LED was developed by applying a phosphor coating to a blue LED. Since then, the development of this technology has been growing until the appearance of the high-power LED that are widely used today in many fields of lighting (Bourget, 2008).

It was also in the '90s that the first UV LED formed with a GaN semiconductor exhibiting a low efficiency of around 1 % was developed by Japanese researchers. GaN is a broadband semiconductor capable of emitting light. It has high electron mobility and high thermal resistance, making it suitable for high-power applications. GaN LED are made by depositing layers of GaN semiconductor material onto a substrate, usually sapphire. The upper layer of the LED structure is a p-type GaN layer, and the lower layer is an n-type. Electrons are injected from the n-shell into the p-type material, and upon recombining with the holes, they emit photons in the visible wavelength range. LED made with GaN have higher energy efficiency, higher durability and a longer lifespan than previously ones. Furthermore, GaN LED can produce light in a wide range of wavelengths. Years after its discovery he first UV LED began to appear in the market, and from 2008, commercial LED began to offer enough power at reasonable prices, opening the possibility of their use in diverse applications in water treatment and showing a very promising future (Heathcote, 2011).

1.2. Features of UV LED light sources

Traditionally, UV light has been generated with mercury lamps, including low-pressure (LP) ones, which emit nearly monochromatic UV light at a wavelength of 254 nm, and medium-pressure lamps (MP), which emit a polychromatic spectrum with various wavelengths (200–600 nm), considered an effective inactivation source of microbial present in water (Keshavarzfathy et al., 2021; Sholtes and Linden, 2019).

The two main advantages of LED over other lighting systems are their high efficiency in converting electricity into light, and their long-life span (> 50,000 h). The radiation that a LED device can emit depends on the manufacturing materials, allowing a wide range of wavelengths, from the UV to the infrared region, available nowadays in the market. In addition, LED are very resistant devices with no fragile glass envelope, and their useful life is not shortened by the repetition of on/off cycles as with other lighting devices, such as incandescent lamps, fluorescent lamps, or arc-discharge lamps. They also avoid the use of dangerous compounds, such as the mercury used in fluorescent lamps (Martín-Sómer et al., 2018), and they are

small in size, allowing great flexibility for the design of light sources in photoreactors.

Despite all these advantages, nowadays, UV LED and especially UVC LED still offer low efficiencies at higher current densities compared to visible LED, limiting their implementation in industrial systems for the moment. However, with the rapid evolution of LED over the years, this issue is expected to be promptly solved. On the other hand, an issue that must be considered is that the lower efficiency of UV LED causes greater heat generation, which can lead to an overheating phenomenon if the photoreactor design is not carried out correctly. Despite this drawback, their efficiency has been highly proven for water treatment with different pollutants, such as phenol (Levchuk et al., 2015), dyes (Martín-Sómer et al., 2020; Natarajan et al., 2011; Repo et al., 2013), water purification (Yin and Shang, 2020), micropollutants removal (Cai et al., 2021; Fujioka et al., 2020; Xiong et al., 2020), metal removal (Liu et al., 2014), inactivation of different bacteria and parasites (Pousty et al., 2021; Takahashi et al., 2020; Thatcher and Adams, 2021), or even for coronavirus inactivation (Gerchman et al., 2020).

The electrical efficiency of the traditional mercury UVA fluorescent lamps used for photocatalytic water treatment is very low, around 15 %. With the development of LED in the UVA range, a promising alternative was opened towards a notable improvement in the efficiency of these processes. However, their low initial efficiency also led to the search for an alternative catalytic material sensitive to near-visible light, a spectral region where LED lighting systems were considerably more efficient (Kim and Kang, 2020; Kim et al., 2020; Xiao et al., 2018). In recent years, the improvement of UVA LED devices has boosted their electrical efficiencies to values between 40 % and 50 %, considerably above those of traditional mercury fluorescent lamps and rapidly approaching that of visible LED. These values are expected to continue increasing in the coming years if their evolution is comparable to that of visible light LED, which will significantly improve their photoactivated water treatment efficiency and the potential implementation on an industrial scale.

On the other hand, UVC light is also especially important in photoactivated water treatment processes, especially those related to the inactivation of microorganisms (Zhang et al., 2021; Lee et al., 2021; Le et al., 2021). At present, the efficiency of LED in the UVC range is still too low (between 1.5 % and 2 %) to consider their widespread use in large-scale processes. However, if their development follows a similar trend to that followed by both visible LED and UVA LED, it is expected that in the next decade, the efficiency of UVC LED devices will exceed that of mercury fluorescent lamps, and they will begin to be considered as viable alternative in industrial systems. Fig. 1 shows the increase in efficiency of LED devices in recent years and the prediction (dashed lines) of the efficiency of UVC LED in the coming years by extrapolating the historical pattern of visible and UVA LED.

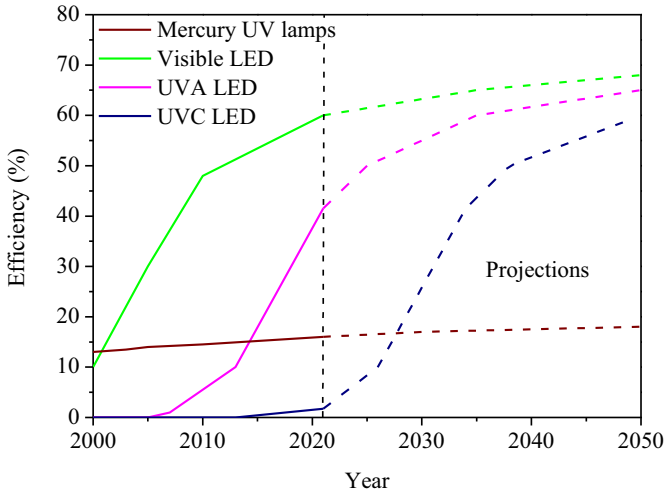

Fig. 1. Efficiency evolution and comparative projections of mercury lamp, visible LED, UVA LED and UVC LED.

1.3. Mechanisms of water disinfection by UV light

It is well known that UVC (100–280 nm) light causes the inactivation of microbial pathogens when their nucleic acids absorb UV photons. These photons trigger damage in DNA molecules by forming cyclobutane pyrimidine dimers (CPD) between consecutive base pairs, inhibiting transcription and replication. Maximum UV light absorption from DNA is reached at a wavelength range of 240–260 nm with a maximum peak at ~260 nm; however, in most cases, the absorption peak wavelength distribution may vary among microorganisms (Chen et al., 2017; Li et al., 2019). In addition, other intracellular components, such as proteins, enzymes, and/or the cell membrane, may be involved in the inactivation mechanism. Therefore, the specific UV absorption spectrum of each pathogen needs to be considered. Table 1 summarises the optimal absorption wavelengths of DNA and other components, such as enzymes and macromolecules, participating in the UV inactivation process. Regarding UVB (280–315 nm) disinfection, it was confirmed, by using the regulator protein *RecA,* that is activated by DNA damage and can be used as an indicator of the potential of bacteria DNA damage restoration caused by UVB, and the gene *SoxS* used as an indicator of oxidative stress. Results point out that the 285 nm and 295 nm wavelengths resulted in more activation of SoxS promoter, probably due to the higher production of reactive oxygen species (ROS) that are known to damage multiple cellular components, including proteins and DNA (Pousty et al., 2021).

The photochemical formation of pyrimidine dimers on DNA is mostly reversible, and the DNA damage can be repaired by the biological processes in the cells (Song et al., 2019a). Most DNA damage can be fixed through photoreactivation and dark repair (Hutchinson et al., 1980), increasing the human health risks of water contamination. Dark repair, in the absence of light, replaces damaged DNA nucleotides with undamaged DNA, whereas photoreactivation is the fixing mechanism under low UV doses. In photoreactivation repair, photoenzymes, e.g., photolyase, present in bacteria have been identified as responsible for the dimers repair by absorbing light in the wavelength range of 315–480 nm (UVA and partial visible light) at low UV doses (below 1500 mJ/cm^2) (Song et al., 2019a). However, UVA has also been reported to cause the inactivation of microorganisms when coupled with UVC (Chevremont et al., 2012; Nyangaresi et al., 2018) by preventing photoreactivation and dark repair. In fact, at high UV doses, UVA can lead to the formation of reactive oxygen species (ROS) in the presence of internal (Fe, 5-formyluracil residues in the DNA molecule, endogenous photosensitisers, e.g., cytochromes) (Song et al., 2019b) or external components (organic matter, H_2O_2) acting as photosensitisers (Li et al., 2019; Aparici-Espert et al., 2018). ROS can attack the cell membrane and other cellular components, increasing the microbial inactivation efficiency due to irreversible damage. In low doses, UVA irradiation has also been reported to induce sub-lethal effects, leading to physiological alterations, e.g., radiation-induced growth inhibition, growth delay, membrane damage, protein oxidation, decreased energy metabolism, and mutation (Song et al., 2019a; Nyangaresi et al., 2018; Song et al., 2019b; Oppezzo and Pizarro, 2001). Sub-lethal effects of UVA radiation at a UV dose below 100,000 mJ/cm^2 have been detected in *E. coli* (Song et al., 2019a). For example, Song et al. (2019b) demonstrated that with UVA pretreatment (17,000–52,000 mJ/cm^2) before UVC exposure, *E. coli* is only photo reactivated up to 15 %, in contrast with 60 % when only UVC treatment was applied. They also confirmed their statements, by adding mannitol to remove $^{\bullet}$OH, that this highly reactive radical played an important role in the UVA pretreatment. As no *E. coli* inactivation was detected during the UVA pretreatment (52,000 mJ/cm^2), it was thought that the hydroxyl radical might only induce a non-lethal effect on *E. coli* by disrupting the bacterial membrane. This would make impaired bacteria more sensitive to subsequent UVC exposure, not enabling them to photo-/reactivate afterwards (Song et al., 2019b), resulting in an

Table 1
Optimal wavelengths (nm) in the range of DNA absorption and other microorganism components responsible for UV inactivation of microorganisms and photo repair.

Microorganism / internal components	Type of microorganism	DNA absorption peak (nm)	Reference
Enteric bacteria (nucleid acid in DNA forming Cyclobutane Pyrimidine Dimers, CPD)	Bacteria	200–300, peak 260	(Gillespie et al., 2017; Hull et al., 2019; Hull and Linden, 2018)
B. pumillus	Spore	260, 270	(Hull et al., 2019; Martino et al., 2020)
B. subtilis	Spore	240, 260, 270	(Gillespie et al., 2017; Martino et al., 2020)
MS2 RNA	Bacteriophage (virus)	230–265, 270–280	(Rattanakul and Oguma, 2018; Oguma et al., 2019; Kojima et al., n.d.; Sholtes et al., 2016)
T2	Bacteriophage (virus)	265	(Zou et al., 2019)
T7	Bacteriophage (virus)	270	(Zou et al., 2019)
ϕX-174	Bacteriophage (virus)	265	(Zou et al., 2019)
Vesicular stomatitis virus	Virus	265	(Zou et al., 2019)
Influenza Virus (IAV) (Viral RNA)	Virus	240–290	(Würtele et al., 2011)
Adenovirus (HAdV)	Virus	230–260, 260–270, 270–280	(Zou et al., 2019; Oguma et al., 2019; Kojima et al., n.d.; Sholtes et al., 2016)
B. subtilis	Spore	263–268	(Zou et al., 2019; Martino et al., 2020)
B. pumillus	Spore	260–268	(Zou et al., 2019; Martino et al., 2020)
HAdV2 (Proteins)	Virus	275–280-285	(Li et al., 2019; Hull et al., 2019; Sholtes et al., 2016)
MS2 (Proteins)	Bacteriophage (virus)	275–280-285	(Li et al., 2019; Hull et al., 2019; Sholtes et al., 2016)
B. pumillus (small acid-soluble proteins bound to the spore DNA)	Spore	220–228 (MP UV)	(Hull et al., 2019)
Cryptosporidium parvum	Protozoa	254–280 (peak 275)	(Zou et al., 2019; Kojima et al., n.d.)
Photolyase enzyme (DNA photo-repair)	Bacteria	310–480	(Gillespie et al., 2017; Song et al., 2018; Sommer et al., 1998; Nguyen et al., 2019; Hull and Linden, 2018)
Repair enzymes	Bacteria	280	(Hull and Linden, 2018)
Promotion of CPD formation in following UVC radiation	Bacteria	365	(Kim and Kang, 2020)
RecA gene expression which combines with CPD and block the pathway of dark repair	Bacteria	365	(Kim and Kang, 2020)
TLS response enhancing the tolerance to DNA damage, declining UmuD protein	Bacteria	365	(Kim and Kang, 2020)

overall improvement in the inactivation. Other possible inactivation mechanisms reported for UVA radiation, in this case for UVA pre-radiation before UVC treatment, are based on the promotion of the CPD formation in the subsequent UVC radiation (Xiao et al., 2018). It has also been reported that UVA radiation could also induce the *RecA* gene expression and the over-production of the *RecA* protein, which could inhibit repair since the *RecA* protein could combine with the CPD and block the pathway of dark repair (Xiao et al., 2018). The translation DNA synthesis (TLS) mechanism should also be considered as a possible mechanism for enhancing UV resistance. If the TLS response was enhanced after UVA exposure, the *UmuD* protein would decline. TLS seemed to be a compensatory survival strategy for UVC disinfection of sensitive strains. Their previous exposure to UVA may increase their resistance to UVC, favouring their tolerance to DNA damage (Xiao et al., 2018). Therefore, the mechanisms for UVA largely relate to biological processes in bacteria rather than direct photochemical reactions on DNA.

On the other hand, in photocatalytic processes there are different inactivation mechanisms based on the formation of oxidising species such as the hydroxyl radical (•OH). Roughly, the photocatalytic processes begin when a photocatalyst, a semiconductor material, is irradiated with a wavelength equal to or greater than its band gap, typically UVA radiation in the 360–390 nm wavelength. The absorbed photons cause the promotion of electrons (e^-) to the conduction band, leaving positive holes (h^+) on the valence band. These charge carriers can recombine, releasing heat, or can reach the surface of the photocatalyst particles and initiate oxidation and reduction reactions (Elgohary et al., 2021). In an aqueous environment, the holes can oxidise adsorbed water molecules generating hydroxyl radicals, which can oxidise, subsequently, organic pollutants or microorganisms producing carbon dioxide, water, and mineral salts (Elgohary et al., 2021). On the other hand, the electrons can be accepted by O_2 generating superoxide species $\bullet O_2$- or other ROS.

Several mechanisms have been proposed in the literature where the generation of ROS by photocatalysts is implicated in bacteria inactivation. The cell membrane can be attacked by ROS (Baaloudj et al., 2021). Also, ROS can enter the bacterial cell causing further oxidation of the internal cellular macromolecular components, such as lipids, proteins, carbohydrates, amino acids, and nucleic acids (DNA and RNA) (Saravanan et al., 2021; Rodríguez-González et al., 2020). ROS damage to the cell membrane and cell wall also leads to the leaking out of internal cellular components, leading to inactivation and bacterial cell death (Deng et al., 2020). Photocatalyst particles can also attack bacterial cells by depositing them on the surface, resulting in the destruction of membrane proteins or cell membranes. Both semiconductor particles and ROS can disturb the transport of electrons in the cell, loss of proton motive force, depletion of intracellular ATP production, DNA replication disintegration, and intracellular outflow resulting in cell death (Ray et al., 2018).

2. New insights into the application of UV LED for water disinfection

2.1. Tunable emission wavelength

As previously described, it has been well established that photons with wavelengths in the range of 240 nm to 280 nm are effectively absorbed by DNA (Chen et al., 2017; Li et al., 2019). Thus, the overlap between the lamp emission spectrum and the absorption spectrum of DNA is a critical factor for UV inactivation. The selection of a UV LED with specific peak emission wavelengths enables the simultaneous optimisation of the DNA absorption spectra of different target microorganisms, which is impossible with mercury lamps (Chen et al., 2017). It also maximises the electrical energy conversion to useful radiation, increasing the electrical efficiency.

In general, the 260–265 nm UV LED has been considered to possess a greater germicidal effect compared to 280 nm, but irradiation with 280 nm was reported to repress photoreactivation (even under low UVA doses of 6.9 mJ/cm^2) and dark repair (Nyangaresi et al., 2018; Li et al., 2017). This means that fewer dimers were repaired after exposure to 280 nm, and instead may be linked to structural damage to some enzymes involved in the DNA repair, such as photolyase (Li et al., 2017) and protein damage caused by the absorbance of the aromatic amino acids tryptophan, tyrosine, and cystine (i.e., of disulfide bonds) (Nyangaresi et al., 2018). This conclusion requires further investigation since, e.g., Shen et al. (2020) described that the percentage of photoreactivation after inactivation by a 268 nm UV LED was slightly less than that of 275 nm when two Gram-positive tetracycline-resistant bacteria (TRB) from *Bacillus* species were irradiated (*Bacillus cereus*, TRB-3, and *B. pumilus*,

TRB-5). However, the damage caused by 268 nm UV on DNA should have been more easily repaired than that by a 275 nm UV LED, which was responsible for protein damage for most bacteria. The reason for this different trend may be the larger size of resistance-associated proteins (> 15,000 Da) in antibiotic-resistant bacteria (ARB), which may require antimicrobial resistance coding genes for them to be expressed. This means that protein damage under 275–280 nm for ARB may be much more complex than that for non-ARB (Shen et al., 2020). Therefore, UVC LED exposure was not enough to completely inactivate antibiotic resistance genes (ARGs) like *tet(L)*, and consequently, antibiotic resistance spreading may occur during storage (under UVA-visible light and dark conditions) (Shen et al., 2020).

Around the same topic, Xiao et al. (2018) observed that the dark repair capacities of four strains of *E. coli* (ATTC 15597, 11229, 25922, 700891) were significantly inhibited after UVA pre-radiation (7200 and 10,800 mJ/cm^2) coupled to a sequential 265 nm UVC LED exposure. However, for all the *E. coli* strains, the photo repair performance was not significantly influenced by UVA pre-radiation. A higher UVA pre-radiation dosage was required (above 7.5×10^8 mJ/cm^2) to lead to the formation of ROS with the ability to affect the bacterial membrane. These results did not agree with those reported by Song et al. (2019b). Indeed, an opposite trend was observed. UVA pretreatment (17,000–52,000 mJ/cm^2) mainly suppressed photoreactivation but hardly affected the dark repair of bacteria. This was explained by the fact that photoreactivation was a simple repair system consisting of only one enzyme, photolyase, as compared to dark repair mechanisms that seemed to be based on multiple pathways and enzymes (Song et al., 2019b).

On the other hand, UVA LED lamps with emissions around 360–390 nm are used in photocatalysed reactions with oxidants and/or catalysts, which can lead to the photogeneration of ROS. In comparison with the photocatalytic disinfection studies performed with traditional UV lamps, there have been few publications on photocatalytic disinfection with UVA LED lamps.

An interesting work by Xiong and Hu (2013) compared the UVA LED/TiO_2 process in antibiotic-resistant bacteria disinfection, both in continuous and periodic illumination with a UVA mercury lamp in the photocatalytic process, and UVC in the photolysis process. The results showed that, after UVC illumination, both photoreactivation and dark repair of *E. coli* antibiotic-resistant bacteria took place in the following 4 h, with dark repair occurring to a much lesser extent than photoreactivation. The bacterial concentration was quite similar after the continuous UVA LED/TiO_2 and UVA mercury lamp illuminated photocatalytic process, probably because the UV wavelength (365 nm) and UV dose (28.8 J/cm^2) were the same. As concerns bacterial regrowth after the UVA mercury lamp or UVA LED/TiO_2 illumination processes, neither photoreactivation nor dark repair was found, since hydroxyl radical oxidation led to bacterial membrane damage and final lysis. On the contrary, the bacterial concentration decreased to an undetectable level within the following 4 h. However, although the comparison between bacterial photoreactivation and dark repair changes was similar with both lamp illumination systems, the calculated electric energy for the UVA mercury lamp (2.88×10^4 J) was much higher compared to that shown by the UVA LED source (194.4 J).

Generally speaking, UVA LED photocatalytic disinfection is poorly studied and very limited to *E. coli*. However, UVA LED with sufficient energy efficiency are already on the market, providing several advantages for implementing photocatalytic disinfection processes based on semiconductor or Fenton processes. In this case, it is not clear that LED improve the efficiency of photocatalysts compared to the use of UVA mercury lamps. In fact, if the light distribution of LED is not optimised, LED can be less effective than traditional lamps (Martín-Sómer et al., 2017). However, although in the case of the degradation of chemicals an improvement is observed when the light distribution is optimised, in the inactivation of bacteria this difference is not evident. In the case of microorganisms, the UV LED dose, light intensity (fluence rate), and exposure time are the most important factors for effective disinfection with photocatalysts and these three factors must be carefully selected.

2.2. Synergistic effect between different wavelengths

One of the main characteristics of electroluminescence is that it is emitted in a very small range of wavelengths, which makes it possible to better select the LED to use for a specific application. The easy choice of wavelength in LED devices allows almost infinite designs for a better bacterial inactivation. Combining the main peak emission with other emission wavelengths may have a synergistic inactivation effect because of the different UV photosensitivity of the microorganisms and/or their components, i.e., enzymes, macromolecules, etc., increasing the effectiveness of the UV inactivation. However, this synergistic effect is still under debate.

No conclusive synergistic effect for microbial inactivation has been observed by combination or sequencing radiation coming from UVC and UVB LED. According to the Second Law of Photochemistry, the photochemical effects of different wavelengths on a molecule should be independent of each other, achieving only as much inactivation or genome damage as the sum of the photonic response from those wavelengths emitting separately. Beck et al. (n.d.) did not observe a synergistic effect of the dual-UVC wavelength (260 + 280 nm) applied to the inactivation of *E. coli*, MS2, HAdV2, and *B. pumilus* spores. This is in agreement with the results reported by Li et al. (2017). Sholtes and Linden (2019) did not demonstrate any synergistic effect either when a 265 (33 %) and 285 (67 %) nm UV LED were either combined or sequentially applied (265–285, 285–265) for *E. coli*, *P. aeruginosa*, and MS2 inactivation. No synergistic effect of 267 + 275 nm, 267 + 310 nm, and 275 + 310 nm was also reported by Nyangaresi et al. (2018) for *E. coli* inactivation. The 267 nm UV LED reached the highest log inactivation, followed by the 267 + 275 nm and 275 nm UV LED. Song et al. (2019a) combined the 265 nm and 285 nm UV LED together and tested both under simultaneous and sequential exposures to inactivate *E. coli*. Their effects also led to the same $\log_{10}$ inactivation, which is statistically comparable with the sum of log inactivation by each wavelength applied alone. Thus, 265 + 285 nm, 265–285 nm, and 285–265 nm always achieved an additive inactivation effect. Betzalel et al. (2020), when combining the 265 + 285 nm UV LED, did not achieve better results in terms of *E. coli* and MS2 inactivation when compared to the individual exposures. The same was stated by Silva et al. (2020) when coupling the 255 + 280 nm UV LED for *E. coli* inactivation in a secondary effluent and subsequently filtered wastewater. These results confirmed the already cited Second Law of Photochemistry.

However, synergistic effects have been observed when combining UVA and UVC irradiation. Differences have also been reported when irradiation was performed simultaneously or sequentially. Chevremont et al. (2012) reported that simultaneously coupling wavelengths of 280 + 365 nm or 280 + 405 nm synergistically enhanced the inactivation efficiency of pure cultured strains of *E. coli* and *Enterococcus faecalis* as well as wild fecal indicator bacteria in treated wastewater. This synergy was reported due to a higher optical output available in the UVA LED as well as the potential for the UVA light to produce reactive forms of oxygen (ROS), such as oxygen free radicals and hydrogen peroxides, through photosensitisation due to the presence of natural organic matter and to react with oxygen dissolved in water. ROS formation led to an additional disinfection mechanism based on oxidative stress compromising the integrity of the bacterial cell wall, which involves irreversible damage and the impossibility of regrowth.

Sequential UVA-UVC or UVC-UVA exposures have also been explored by Xiao et al. (2018). UVA pre-radiation with UV doses of 7200 mJ/cm^2 (365–265 nm) enhanced the inactivation performances (synergistic effect) of *E. coli* ATCC 11229, ATCC 15597, and ATCC 700891 by at least 0.5 $\log_{10}$ in comparison with only 265 nm UVC LED radiation. When the UVA pre-radiation time was increased (10800 mJ/cm^2), the inactivation performance was promoted by 2 $\log_{10}$ (ATCC 15597), 1 $\log_{10}$ (ATCC 11229), and 2 $\log_{10}$ (ATCC 700891). It is important to note that *E. coli* ATCC 700891 is known as an antibiotic-resistant (ampicillin and streptomycin) strain that is quite resistant to UV disinfection. On the contrary, UVA pre-radiation caused a detrimental effect of at least 0.5 $\log_{10}$ only for *E. coli* ATCC 25922, suggesting that it was more resistant to UVC after UVA pre-radiation. In this case, the enhanced CPD formation during UVA pre-

irradiation was found to be the cause of the greater inactivation performance observed for *E. coli* 15597, 11229, and 70089. The strong TLS response detected for UV-sensitive strains, as is the case of *E. coli* 25922, explained the observed increased resistance to UVC disinfection when this strain is exposed to UVA prior to UVC exposure (Xiao et al., 2018). Song et al. (2019a, 2019b) also reported the synergistic effect of sequential UVA to UVC exposure (365–265 nm), showing a UVA dose threshold effect. The threshold for 365 nm UVA pretreatment to affect *E. coli* was between 1,700 and 17,000 mJ/cm^2. Hence, this research group confirmed that an increased UVA dose of 17,000–52,000 mJ/cm^2 (10–30 min) significantly improved the overall *E. coli* inactivation. Thus, damaged *E. coli* cells after UVA exposure are probably more vulnerable to subsequent UVC inactivation, enhancing the *E. coli* inactivation. However, combining UVA with UVC simultaneously or applying UVA after UVC (265 + 365 nm, 265–365 nm) reduced the inactivation of *E. coli* due to DNA repair and the photoreactivation effect of UVA at low UV doses. Thus, the energy from UVA radiation was probably used by the enzyme photolyase in bacteria such as *E. coli* to repair UVC-induced DNA damage. In contrast, no significant difference was observed between simultaneous and sequential exposures for MS2 inactivation, and the result is the sum of that obtained by each wavelength alone. No additional effect of the UVA exposure on MS2 is due to the absence of such biological processes in the viruses. Thus, bacteriophages and viruses such as MS2 exhibited only a photochemical effect on DNA or RNA following the Second Law of Photochemistry (Song et al., 2019a; Song et al., 2019b). On the contrary, Silva et al. (2020) did not observe DNA photoreactivation by simultaneous exposure to the UVA LED (365 and 405 nm) and UVC LED (255 and 280 nm).

Regarding combinations of UVB and UVA LED, Song et al. (2019a) reported statistically lower *E. coli* inactivation when testing simultaneous and sequential combinations of UVB- and UVA LED (285 + 365 and 285–365 nm) in comparison with the sum of the inactivation achieved by each wavelength separately. *E. coli* counts recovered slightly upon 365 nm exposure, which was equivalent to a low UV dose of 1160 mJ/cm^2 after a noticeable concentration reduction at 285 nm exposure. When applying 365 nm followed by 285 nm exposure (365–285 nm), the *E. coli* concentration continuously decreased once the 285 nm UV LED irradiation started, but no synergistic effect was detected.

In this sense, in the studies published on photocatalysis where LED lamps are used, no combinations of various wavelengths used simultaneously or sequentially have been found. This would be an interesting research topic since, by combining UVC or UVB with UVA wavelengths, photochemical and photocatalytic inactivation mechanisms could be involved.

2.3. Pulsed radiation

Another advantage of LED devices is the absence of a warm-up time, which allows them to be turned on and off in very short intervals of time. With the help of controllers, the LED can be programmed with pulse lighting in a practically unlimited frequency range, which also brings a potential reduction in energy consumption and control of the thermal management. This type of lighting strategy has been studied in various investigations with the aim of increasing the energy efficiency in inactivation processes, since the use of high intensity pulses can promote greater damage to microorganisms, although the results obtained are not entirely clear (Sholtes and Linden, 2019; Zou et al., 2019; Gillespie et al., 2017; Nyangaresi et al., 2019a). In general, not many studies have evaluated UV LED pulsed radiation, and the results have been somewhat inconsistent, which is probably due to the different UV dose determination methods for continuous and pulsed irradiation. Song et al. (2018) evaluated the advantage of turning the radiation on and off using UV LED, providing pulsed irradiation with flexible pulse patterns. Adjusted pulsed operation of UV LED was recommended instead of using a calculated operation time to deliver an equivalent UV dose.

Two main variables are often evaluated, such as the pulse frequency, which is the number of pulse periods per unit of time, and the duty cycle, which is the proportion of turned-on time of the LED during a pulse period (Zou et al., 2019). No significant difference in the log inactivation between the continuous and pulsed irradiation with various frequencies from 0.1 to 1000 Hz has been detected in most studies (Song et al., 2018). Zou et al. (2019), Song et al. (2018), and Sholtes and Linden (2019) also observed that the pulse frequency had little impact on the temperature control of the UV LED in pulsed irradiation. Regarding the effect of the duty cycle on bacterial inactivation for the same UV dose, Zou et al. (2019) observed that the $\log_{10}$-inactivation of *E. coli* increased with the decrease of the turned-on time of the cycle from 100 % to 5 % when using 285 nm UV LED pulsed radiation. However, the time of exposure to keep the same UV dose also increased by a factor of 10, which led to balancing the energy and time efficiency when applying pulsed UV LED irradiation. In fact, they quantified lower energy requirements to achieve a $\log_{10}$ reduction for P285–5 % (10.4 $\log_{10}$/J) compared to continuous radiation (5.3 $\log_{10}$/J). In terms of inactivation efficiency, P285–5 % was also superior, exhibiting a 5 $\log_{10}$ reduction in comparison to the 3 $\log_{10}$ reduction reached by a continuous irradiation source. They also studied the effect of the UV LED wavelength, which led to a 2.5 $\log_{10}$ *E. coli* inactivation for the continuous irradiation of both 280 and 265 nm at a total UV dose of 10 mJ/cm^2 and UV fluence rate of 0.04 W/m^2. Above that UV dose, differences between pulsed and continuous radiation became more obvious (Zou et al., 2019). When a 5-fold current (100 mA vs 20 mA) pulse radiation for 285 nm (5 %, 1000 Hz) was applied with a fluence rate of 0.03 mW/cm^2, pulsing radiation showed a much higher inactivation efficiency than continuous one. However, the higher current led to an extra increase in energy consumption of 1.3 times, making not viable in terms of energy consumption.

On the contrary, Song et al. (2018) confirmed that the 265 nm UV LED continuous and pulsed irradiation reached comparable *E. coli* and MS2 inactivation at various frequencies and duty rates. Sholtes and Linden (2019) did not find statistically significant differences among pulsing conditions (265 and 285 nm UV LED with duty rates ranging from 10 to 90 %) and continuous irradiation for *E coli*, *P. aeruginosa*, and MS2 inactivation. Thus, the results followed the Bunsen–Roscoe Reciprocity Law, since the biological impacts due to a specific UV dose were directly proportional to the total UV dose delivered, independently of the regime in which it was applied. Nyangaresi et al. (2019a) reported that, for xenon lamps pulsed UV irradiation, disinfection can be achieved through bacterial membrane disruption due to overheating only with UV doses exceeding 500 mJ/cm^2. Thus, considering the significantly low output power of the current UVC LED compared to that of xenon lamps, the stress on the cells from UVC LED pulsed irradiation is probably not enough to cause either photophysical or photothermal damage to the cells (Song et al., 2018). However, operation in pulsed irradiation at a 50 % duty rate with various frequencies reduced the rate of the temperature rise, e.g., the temperature reached 45 °C after running for 25 s in pulsed radiation compared to 50 °C after 15 s for continuous radiation.

On the other hand, the use of pulsed lighting has also been considered in photocatalytic processes. Photocatalytic reactions are initiated by the absorption of photons by the photocatalyst, which triggers the generation of free electron-hole pairs. This is a very fast process, of the order of femtoseconds (Xiong and Hu, 2017), compared to the rest of the subsequent reactions that take place until the oxidation of the pollutants. These downstream reactions occur in nano to millisecond time frames and do not require light for them to occur. For this reason, a strategy to increase the energy efficiency of the process is the use of pulses with suitable duration to generate the electron-hole pairs, followed by dark stages for the rest of the subsequent reactions that do not need light (Tokode et al., 2016). In this way, while increasing the energy efficiency, it is possible to improve the quantum efficiency of the photocatalyst due to the limitation in the production of the hole electron pairs that significantly reduce the recombination phenomena (Levchuk et al., 2015). This strategy, which a priori seems very beneficial in terms of energy improvement, has not yet been studied in depth (Bertagna Silva et al., 2021), so it is one of the main fields to be developed in the near future to achieve the implementation of LED systems at the industrial level.

In the photocatalytic process, two factors that affect the photocatalytic inactivation of antibiotic-resistant bacteria have also been studied: the cycle time, defined as one cycle "on" and "off" time and, the duty cycle, calculated as "on"/("on + off") (Xiong and Hu, 2013). The effect of the cycle time demonstrated that with the increase of cycle time from 20 ms to 2000 ms, the log-removal decreased from 1.26 to 0.54 with a UVA dose of 33.6 J/cm^2 and a fluence rate of 80 W/m^2. Regarding the effect of the duty cycle, log-removal decreased substantially with the increase of the duty cycle from 0.25 to 4 using the same UVA dose, although at low UVA dosages (0–30 mJ/cm^2), log removals in the initial stage were found to be quite similar under continuous and periodic illuminations. However, with further increase of the UVA dose, more log-removal was found under the 0.25 duty cycle. This phenomenon is explained by the fact that with a low UVA dose, bacteria are still in the delay region, and can recover themselves if given enough dark time. With a high cumulated UVA dose, however, bacteria have some serious damage which makes them less able to recover, and the residual disinfecting effect would kill them during the longer dark period.

2.4. UV dose, fluence rate and wavelength

Two important factors to consider in UV water disinfection processes are the UV dose and the fluence rate. UV inactivation is expected to follow the Time–Dose Reciprocity Law (or the above-mentioned, Bunsen–Roscoe Reciprocity Law), which states that the photochemical effect depends only on the total energy dose, regardless of the UV fluence rate. However, deviations from the Reciprocity Law occur, exhibiting higher log inactivation at a higher fluence rate and shorter exposure time than under a lower fluence rate and prolonged exposure time for the same total UV dose. This effect was attributed to repair enzymes in bacteria, which became more severely impaired by a high fluence rate. This phenomenon could suggest that UV water disinfection depends on both photochemical reactions and biological processes (Xiong et al., 2020; Hutchinson et al., 1980; Sommer et al., 1998). Pousty et al. (2021) described the effects of the fluence rate for *E. coli* inactivation for 265, 275, 285, and 295 nm UV LED. The fluence rate did not have any impact on the inactivation kinetics for the 265 nm UV LED. For example, for a total UV dose of 8 mJ/cm^2, a similar 4.58 $\log_{10}$ reduction was observed for a low fluence rate (0.012 W/m^2) with a long exposure time (6670 s) and a high fluence rate (1.1 W/m^2) with a short exposure time (69 s). Thus, for this wavelength, *E. coli* inactivation followed the Time–Dose Reciprocity Law. On the contrary, a different trend was obtained for longer UV LED wavelengths, becoming more noticeable at the longest UV LED wavelength tested. Hence, for the 275, 285, and 295 nm UV LED, a higher log inactivation was achieved at a lower fluence rate and a longer exposure time. Therefore, as the UV LED wavelength increased, the deviation from the Time–Dose Reciprocity Law become higher. This finding correlated with higher activation of the *SoxS* promoter for longer wavelengths, leading to greater production of ROS. These ROS are responsible for affecting biological processes in the cells rather than inducing photochemical reactions in DNA. In conclusion, bacterial inactivation depended not only on the UV dose (mJ/cm^2) but also on the average fluence rate (mW/cm^2 or W/m^2), and the wavelength used.

In addition to this, several researchers observed that the high radiation flux and short exposure time result in a higher logarithmic inactivation compared with a low flux and long exposure time, as prolonged exposure times may cause microbial aggregation, which leads to decreased inactivation (Lee et al., 2018; Zhou et al., 2017; Nguyen et al., 2019).

Research results with other microorganisms have been reported by Kim et al. (2017), who achieved 1 $\log_{10}$ reduction of MS2, Qβ, and ϕX174 inactivation by applying a UV dose at 266 nm ranging between 0.14 and 1.29 mJ/cm^2 compared to a UV dose of 2.14 to 2.43 mJ/cm^2 required for LP UV lamps. Li et al. (2017)) also reported a higher efficiency for *E. coli* inactivation for a 265 nm UV LED over LP UV. The same results were reported by Sholtes and Linden (2019)) for *E. coli*, *Pseudomonas aeruginosa*, and MS2 inactivation, and Hull et al. (2019; Hull and Linden, 2018) reported the same for MS2 inactivation. In this case, UV dose values for 1 $\log_{10}$ inactivation corresponded to 13.33, 16.65, and 33.3 mJ/cm^2 for 255, 266, and 285 nm UV LED, respectively, and 20 mJ/cm^2 for LP UV lamps. The results confirmed that wavelengths of 255–265 nm closer to the DNA absorption possess a higher germicidal effect (Sholtes and Linden, 2019). The results provided by Betzalel et al. (2020) and Li et al. (2017) did align with higher *E. coli* inactivation for the 265 nm UV LED compared to 280 nm. As expected, the 260 nm UV LED was much more efficient than 280 nm for MS2 inactivation since the UV absorbance of MS2 RNA and the MS2 action spectrum both have a relative peak near 260 nm (Beck et al., n.d.; Betzalel et al., 2020; Hull et al., 2019). The UV LED of 255, 265, and 285 nm were also tested by Martino et al. (2020) for *E. coli* and bacteriophage P22 inactivation. Higher inactivation efficiencies were attained by 255 nm and 265 nm in comparison with 285 nm, as expected. Kim et al. (2017) also reported a higher inactivation efficiency for MS2, Qβ, and ϕX174 when using 266 nm against a 279 nm UV LED.

Rattanakul and Oguma (2018) reported a comparison of the UV dose required for the inactivation of 1 $\log_{10}$ of different bacteria and bacteriophages for different UV radiation sources, reporting fluence values as follows:

- LP UV: 1.23 (*E. coli*), 1.51 (*Legionella pneumophila*), 2.22 (*Pseudomonas aeruginosa*), 11.76 (Qβ).
- 265 nm UV LED: 1.16 (*L. pneumophila*), 1.23 (*E. coli*), 1.33 (*P. aeruginosa*), 10.20 (Qβ).
- 280 nm UV LED: 1.78 (*E. coli*), 1.96 (*P. aeruginosa*), 2.22 (*L. pneumophila*), 17.86 (Qβ).

Again, the 265 nm UV LED provided the best performance in terms of microorganism inactivation. Similar values of UV dose per inactivated $\log_{10}$ were reported (Oguma et al., 2019) for the 265 nm UV LED, which was superior to 280 nm UV LED inactivation: 1.06 /2.2 (*L. pneumophila*); 1.63/2.43 (*E. coli*); 1.7/2.0 (*P. aeruginosa*); 2.83/3.93 (*Vibrio parahaemolyticus*); 8.17/9.63 (*Feline calcivirus,* FCV); 10.3/18.0 (Qβ); 25.37/30.5 (MS2) mJ/cm^2/$\log_{10}$ for the 265 and 280 nm UV LED, respectively. Concerning inactivation of antibiotic resistant bacteria, Shen et al. (2020) reported UV doses required to achieve 1 $\log_{10}$ reduction when using the 268 and 275 nm UV LED when comparing TRB-3 and TRB-5 to non-antibiotic-resistant *E. coli*. The obtained values led to a similar UV dose for inactivating antibiotic-resistant microorganisms for both wavelengths (268 and 275 nm), i.e., 2.80 (TRB-3) and 2.70 (TRB-5) mJ/cm^2. Similar values of the UV dose were found for non-resistant *E. coli* for 268 nm (2.88 mJ/cm^2), although differences appeared for the 275 nm UV LED inactivation (5.76 mJ/cm^2). Regarding viruses such as the Influenza A viruses (IAVs), Kojima et al. (n.d.) stated that the 260–290 nm UV LED and LP UV could damage viral RNA, leading again to the 260 nm UV LED having the greatest effects on both the disinfection rate and damage of viral RNA. In fact, they determined the relationship between the absorbance spectrum of viral RNA and the emission spectrum of UV irradiation by calculating a correlation coefficient (R_{AE}) between the normalised absorbance spectrum of viral RNA and the normalised emission spectrum for the UV LED and LP-UV lamp. A higher R_{AE} score corresponded to better disinfection. The values of R_{AE} corresponded to 11.1 (LP UV), 68.2 (260 nm), 42.2 (270 nm), and 86.3 (258.5 nm + 260 nm + 270 nm). Thus, the wider range of the emission spectra of the UV LED as compared to the LP UV lamp was an important advantage for the inactivation of IAVs and the induction of RNA damage (Kojima et al., n.d.).

Differences were observed also between the LP UV lamp and 260 nm UV LED for *Bacillus atrophaeus*, requiring UV doses of 30 and 19 mJ/cm^2, respectively, to achieve 4 $\log_{10}$ reduction (Sholtes et al., 2016). Since *Bacillus* spores exhibit absorption peaks at around 260 and 270 nm, it makes them more sensitive to those wavelengths produced by the LED than the lower 254 nm produced by the LP UV lamp (Würtele et al., 2011). The higher UV dose required to inactivate the spores may also be due to the ability of the spores to aggregate, which allows them to be protected by UV radiation. Beck et al. (n.d.) also found a higher efficiency for *Bacillus pumilus* spore

inactivation with a 260 nm UV LED than with a 280 nm UV LED, which correlates with their action spectrum, showing a greater sensitivity at 260 nm. The results also agree with the studies by Rattanakul and Oguma (2018)) and Oguma et al. (2019), who determined a UV dose of 10.10 (LP UV), 5.74–7.2 (265 nm), and 9.6–12.1 (280 nm) mJ/cm^2 per log inactivated of *Bacillus subtilis*.

Also, the 285 nm UV LED was also much more efficient in the inactivation of high UV-resistant adenovirus serotype 5 (43.5 mJ/cm^2/log inactivation) in comparison with the LP UV lamp (50 mJ/cm^2/log inactivation) (Oguma et al., 2016). In this case, the inactivation mechanisms may be attributed to protein damage, as proteins show an absorption peak at around 280 nm, with irreversible effects for DNA repair mechanisms in the host cell (Beck et al., n.d.; Oguma et al., 2016). Beck et al. (n.d.) also reported this finding, and observed that the MP UV lamp was most effective for adenovirus serotype 2 (HAdV2) and *Bacillus pumilus* spores. A similar finding was reported by Keshavarzfathy et al. (2021) for adenovirus serotype 5 (15 mJ/cm^2/log inactivation). Since MP UV emits at low wavelengths, including from 220 to 228 nm, damage to small acid-soluble proteins bound to the DNA of the spore may occur, noticeably affecting *B. pumilus* spore inactivation. That may also explain the low adenovirus serotype 5 inactivation efficiency obtained by Keshavarzfathy et al. (2021) for an optimised 265 nm UV LED flow-through reactor at a flow rate of 60 L/h (46.5 mJ/cm^2/log inactivation).

Hence, we can compare the inactivation of several pathogens as follows when using the LP UV lamp and the 260–265 nm UV LED: ϕX174 > *E. coli* β > *E. coli K12* > *E. faecalis Bacillus subtilis* > Qβ ≥ MS2 > human adenovirus (HAdV) > *B. pumilus*.

Fig. 2 depicts the commented UV dose values reported to achieve 1 $\log_{10}$ reduction at different UVC LED wavelengths in comparison with LP and MP UV lamps for the inactivation of different types of microorganisms such as bacteria *E. coli* (A), bacteriophage (B), viruses, and *Bacillus* according to different results found in the literature from 2016 and 2021.

Similarly, Table 2 shows the UV dose required to reach 1 $\log_{10}$ reduction, the fluence rate, linear inactivation kinetic constants, and reactor operation mode for different wavelengths and combinations depending on each type of microorganism, for all evaluated reports from 2016 to 2021.

On the other hand, when photocatalysis was used for disinfection, there was a generally observed linear increase in the inactivation of microorganisms with the increase of the fluence rate (Xiong and Hu, 2013; Yan et al., 2018). Yan et al. (Yan et al., 2018) studied the effect of the fluence rate on the disinfection efficiencies of *E. coli* with N-doped TiO_2 material supported, and they observed that a rapid inactivation occurred at a high fluence rate, but no significant increase was observed when the fluence rate exceeded 400 W/m^2. Nyangaresi et al. (2019b) compared the irradiance of the 365 nm UV LED at 4.9–19.8 W/m^2. For the samples without TiO_2 (1 g/L), the inactivation was greatly accelerated as the irradiance increased. The log inactivation of 1.3, 1.6, 2.0, and 2.6 at a fluence rate of 4.9, 9.7, 14.8, and 19.8 W/m^2 was obtained after 40 min, respectively. For samples with TiO_2, the log inactivation was 4.1, 4.3, 4.7, and 5.0 at a fluence rate of 4.9, 9.7, 14.8, and 19.8 W/m^2, respectively. The main difference was that in the photocatalytic process, the inactivation rate increased, and the shoulder length was shortened as the fluence rate increased due to a huddle effect, even expected at a low irradiance, which will prevent the self-defense and auto-repair mechanisms of the *E. coli* bacteria from protecting the cells.

2.5. Electrical consumption/efficiency

Electrical consumption per order ($E_{E,O}$) is defined as the amount of electrical energy required to reduce the concentration of microbes by one order of magnitude in a specific volume of water. For direct UVC bacterial inactivation, it is important to note that LP and MP UV systems are still much more efficient in converting input energy to germicidal output compared with UVC LED ($E_{E,0}$ < 0.1 kWh/m^3) (Martino et al., 2020). Among the tested wavelengths, the ~260 nm UVC LED seemed to achieve the highest bacterial inactivation, regardless of the bacterial species, which correlated with the highest UV absorbance of nucleic acids at ~260 nm. However, because of the low wall plug efficiency (WPE) reported for the UVC LED of this wavelength (<10 %) (Song et al., 2018), most of the input power was transformed in heat during the operation of the UV LED. Thus, the 280 nm wavelength was an optimum choice to achieve a high inactivation efficiency with minimum energy consumption due to the current stage of the development of the UVC LED. In general, UV LED with shorter wavelengths present lower quantum efficiencies and produce lower optical power outputs than those generated by UV LED with longer wavelengths at the same current. The WPE, which is defined as the ratio of the radiant flux (total optical output power of the device) to the input electrical power, is correlated with this finding (Li et al., 2019; Nyangaresi et al., 2018; Martino et al., 2020; Lawal et al., 2018).

Beck et al. (n.d.)) observed that LP UV lamps followed by MP UV lamps led to the lowest electrical energy per order, i.e. the lowest amount of energy per log reduction for *E. coli* (0.006 and 0.013 kWh/m^3, respectively), similarly for MS2 coliphage and adenovirus HAdV2A. They also confirmed that the 280 nm LED and the 260 + 280 nm LED combination required statistically less energy per log reduction (0.347 and 0.379 kWh/m^3, respectively) than the 260 nm LED (0.464 kWh/m^3) in the case of *E. coli* inactivation. Similar conclusions were obtained by Rattanakul and Oguma (2018) for all tested microorganisms (*E. coli*, *P. aeruginosa*, *L. pneumophila*, bacteriophage Qβ, and *B. subtilis* spores) according to the $E_{E,3}$ values, the electrical energy consumption required for 3 $\log_{10}$ inactivation. The lowest $E_{E,3}$ values corresponded to the LP UV lamps ranging from 0.006 to 0.064 kWh/m^3, and again, the 280 nm UV LED resulted in a better performance compared to the 265 nm UV LED ($E_{E,3}$ = 0.41 kWh/m^3 for 265 nm compared to 0.17 kWh/m^3 for 280 nm for *E. coli*), attributed to the highest WPE given by the 280 nm UV LED. The same tendencies were confirmed for MS2 inactivation (Hull and Linden, 2018), leading to $E_{E,O}$ values of 0.037 kWh/m^3 for the LP UV lamp, meanwhile, the 255, 266, and 285 nm UV required one order of magnitude more energy for equivalent disinfection. These results agreed with typical WPE values of LP UV of 30–35 % (Jarvis et al., 2019). Nyangaresi et al. (2018) also showed that the 275 nm UV LED required the lowest electrical energy dosage for 1 $\log_{10}$ reduction of *E. coli*, with values for $E_{E,O}$ of 0.1367 kWh/m^3 in comparison with other wavelengths and combinations such as 267, 310, 267–275, 267–310 and 267–310 nm UV LED, which again was attributed basically to the highest WPE provided by the 275 nm UV LED. Values of $E_{E,O}$ were also reported by Sholtes and Linden (2019) for the 265 and 285 nm UV LED inactivation experiments: 0.014/0.081 (*E. coli*), 0.058/0.023 (*P. aeruginosa*), and 0.170/0.867 (MS2), respectively. In this case, the electrical efficiency of the 285 nm UV LED did not overcome the relative proximity of the 265 nm UV LED to the absorption spectra for *E. coli* and MS2, opposite to *P. aeruginosa*, which exhibits high photosensitivity to all wavelengths. Thus, the wall plug efficiency must be increased in the next few years from the current levels of <5 % to 35 % (Martino et al., 2020) to consider the UVC LED technology competitive at a large scale compared with the conventional LP and MP UV-based disinfection for water.

A different scenario appeared when bacterial disinfection was carried out using processes driven by UVA or visible light. As shown in Fig. 1, LED in the UVA range already had conversion efficiencies of electricity into light larger than mercury lamps. Therefore, in these cases, the current use of LED devices is highly recommended. In this regard, it is important to consider that, as for UVC LED, higher wavelength LED in the UVA range have greater energy efficiency than those with shorter wavelengths. For this reason, it is important to know the absorption spectrum of the catalyst and carefully select the wavelength to be used in the process, considering both the range of maximum radiation absorption and the range of maximum LED efficiency. Recently, a study was carried out in which LED with emission wavelengths of 365, 385 and 405 nm were used to carry out bacterial disinfection using both a photocatalytic process with TiO_2 and a photo-Fenton process with iron citrate (Martín-Sómer et al., 2018). The results showed that, in the case of TiO_2, due to its large absorption difference at 365 nm, this wavelength, globally, was the most energy-efficient despite

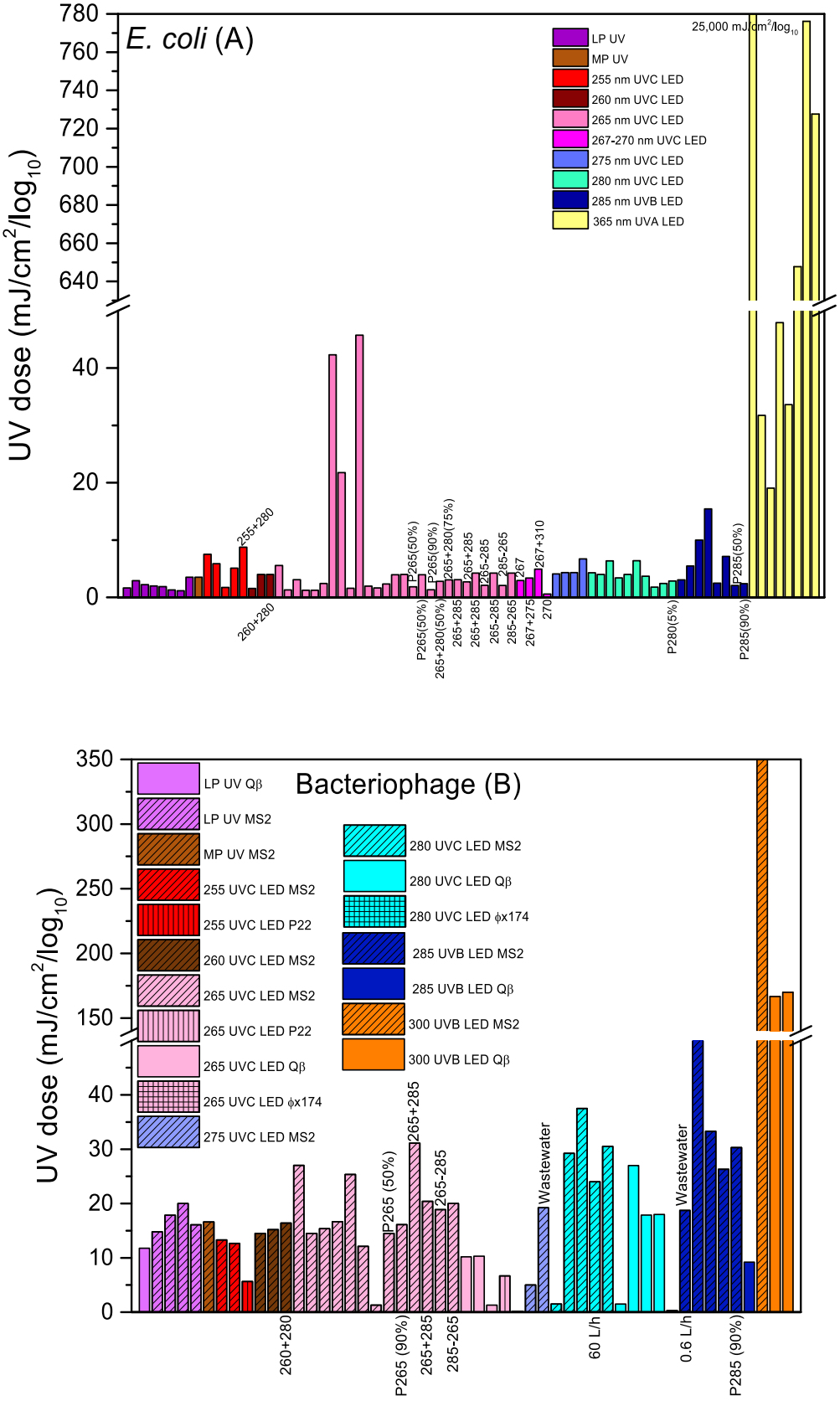

Fig. 2. Comparison of bacteria *E. coli* (A), bacteriophage (B), virus (C), and *Bacillus* spore (D) inactivation efficacy in terms of UV dose required for 1 $\log_{10}$ reduction using UV irradiation (Low-pressure UV, LP UV; Medium pressure UV, MP UV; and UV LED). HAdV2: Adenovirus serotype 2; HAdV5: Adenovirus serotype 5; FCV: Feline Calcivirus. P: Pulsed radiation. Data were taken from references shown in Table 2.

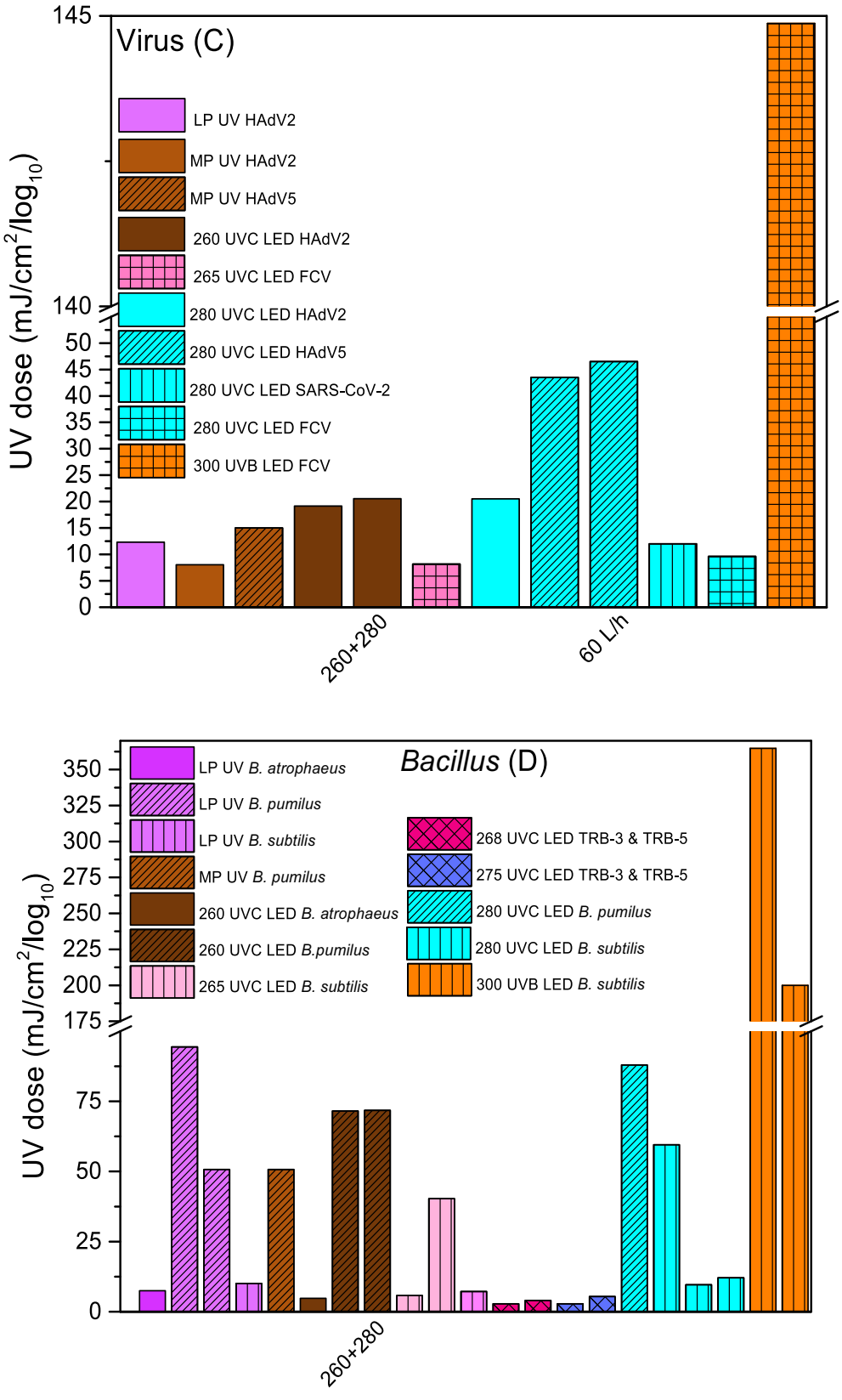

Fig. 2 (*continued*).

the lowest efficiency in converting energy into light. However, in the case of iron citrate, where the drop in absorption with increasing wavelength was not so pronounced, so, the use of the three studied wavelengths led to comparable results in terms of energy consumption.

2.6. System design

Few studies have dealt with the integration of LED systems in reactors even though their use presents great differences from traditional light

Table 2
UV dose responses for 1-log inactivation and inactivation kinetic constants obtained for UV LED disinfection processes.

Wavelength (nm)	Fluence rate (W/m^2)	Microorganism	Log-linear kinetic constant (cm^2/mJ)	UV Dose response per log inactivation (mJ/cm^2)	Reactor	Water matrix	Ref.
LP UV, 260	14,147 (LP UV), 4158 (260)	*Escherichia coli β (ATCC 13033)*, MS2, *Bacillus atrophaeus*	–	1.55 (bacteria); 14.5 (bacteriophague); 4.75 (spore)	Batch, 2 mL total volume, 1.58 mm depth	Phosphate Buffer Saline (PBS)	(Martino et al., 2020)
285 ± 5	2643 (LP UV), 8.87 (285)	*E. coli* K12 IFO 3301, MS2 (ATCC 15597 B1) and Qβ (ATCC 23631 B1), adenovirus 5 (HAdV5) (ATCC VR5)	LP UV/285: 0.505/0.157 (*E. coli*); 0.086/0.037 (Qβ); 0.041/0.029 (MS2); 0.020/0.023 (adenovirus 5)	LP UV/285: 2.0/6.4 (*E. coli*); 11.6/27.0 (Qβ); 24.4/37.5 (MS2); 50.0/43.5 (adenovirus 5)	Batch, 50 mL total volume, 2 mm depth	PBS	(Sholtes et al., 2016)
256, 262, 268, 274, 278 ± 11–256 + 262, 262 + 268, 268 + 274, 274 + 278	–	Algae *Asterionellopsis glacialis*	0.015 (256); 0.0017 (256 + 262); 0.004 (262); 0.0015 (262 + 268); 0.0011 (268); 0.012 (268 + 274); 0.0015 (274); 0.0014 (274 + 278); 0.0015 (278)	253.5 (256); 535.2 (256 + 262)	Batch, 5 mL total volume, 1/3 mm depth	Simulated sea water (salinity 30.6 PSU)	(Kheyrandish et al., 2018)
LP UV, MP UV, 260 ± 12.6, 280 ± 9.8, 260 + 280	3.0–7.5 (LP UV), 3.5–11.7 (MP UV), 1.9–5.5 (UV LED)	*E. coli* K12 (ATCC 29425), MS2 (ATCC 15597-B1), adenovirus 2 (ATCC VR-846), and *Bacillus pumilus* spores (ATCC 27142)	0.27 (LP UV, MP UV), 0.29–0.32 (260, 280, 260 + 280) (*E. coli*); 0.056 (LP UV), 0.061 (MP UV), 0.066 (260), 0.052 (280), 0.061 (260 + 280) (MS2)	3.33–3.67 (LP UV, MP UV), 4 (260; 280; 260 + 280) (*E. coli*); 17.85 (LP UV), 16.4 (MP UV), 15.2 (260), 19.25 (280), 16.4 (260 + 280) (MS2);18.45 (LP UV), 8.05 (MP UV), 19.15 (260), 20.5 (280), 20.55 (260 + 280) (Adenovirus 2); 94.4 (LP UV), 50.7 (MP UV), 71.55 (260), 87.95 (280), 71.8 (260 + 280) (*B. pumillus*)	Batch, 5 mL total volume, 6 mm depth	PBS	66
LP UV, 266 and 279[a]; 279[b]	–[a]; 2546[b]	MS2 (ATCC 15597-B1), Qβ (ATCC 23631-B1) and ϕX 174 bacteriophages (ATCC 13706-B1)	–	2.4 (MS2), 2.3 (Qβ), 2.14 (ϕX 174) (LP UV); 1.29 (MS2 and Qβ), 0.14 (ϕX 174) (266); 1.5 (MS2 and Qβ), 0.33 (ϕX 174) (279) [a]	Batch (10 mL total volume)[a] / Continuous (6 and 18 L/h), retention time of 5.2 and 1.7 s respectively [b]	Distilled water	(Nyangaresi et al., 2019b)
LP UV, 265 ± 10, 280 ± 10, 265 + 280 (50 %), 265 + 280 (75 %)	1.1 (LP UV); 0.5 (265); 1.0 (280); 0.65 (265 + 280 (50 %)); 0.90 (265 + 280 (75 %))	*E. coli* CGMCC 1.3373	0.35 (LP UV); 0.41 (265); 0.30 (280); 0.36 ((265 + 280 (50 %)); 0.32 ((265 + 280 (75 %))	2.86 (LP UV); 2.42 (265); 3.41 (280); 2.79 ((265 + 280 (50 %)); 3.06 ((265 + 280 (75 %))	Batch, 5 mL total volume, 10 mm depth	PBS	(Nguyen et al., 2019)
255 ± 11.3	0.35	*E. coli* (ATCC 15597)	DWK: 0.1605 (UV), 0.1887 (US/UV); SE: 0.1027 (UV), 0.1189 (US/UV)	Distilled water with kaoline (DWK): 7.5 (UV), 5 (US/UV); Secondary effluent (SE): 10 (UV), 8 (US/UV)	Batch: 30 mL total volume	Distilled water (DW) (31.5–33.1 NTU); DW with 20 mg/L kaolin (DWK) (77.4–74.4 NTU); and secondary effluent (SE) (1.91–2.68 NTU)	(Sun et al., 2006)
270 ± 10, 310 ± 10, 365 ± 10, 385 ± 11, 405 ± 13	0.17 (270), 0.085 (310), 120 (365), 490 (385), 650 (405)	*E. coli K12* (ATCC W3110), *Enterococcus faecalis* (ATCC 19433)	–	270/310/365/385/405: 0.58, 160, 25,000, 61,000, 86,000 (*E. coli*); 4.7, −42,000, 42,000, 81,000, 130,000 (*E. faecalis*)	Batch: 1.3 L total volume, 120 mm depth	0.05 M NaCI solution	(García-Gil et al., 2019)
365/265	60 (365), 1.27 (265)	*E. coli* ATCC 15597, ATCC 25922, ATCC 700891, ATCC 11229	–	ATTC 15597/11229/25922/70-0891: 42.3, 21.77,1.59, 45.72 (265); 31.75, 19.05,	Batch: 15 mL, 10 mm depth	Tris-buffered saline (TBS)	(Kim and Kang, 2020)

(continued on next page)

Table 2 (*continued*)

Wavelength (nm)	Fluence rate (W/m^2)	Microorganism	Log-linear kinetic constant (cm^2/mJ)	UV Dose response per log inactivation (mJ/cm^2)	Reactor	Water matrix	Ref.
				47.92, 33.62 (365/265)			
265, P265	5.20 (265), 5.14 (P265, 0.1 Hz, 50 %), 5.36 (P265, 1 Hz, 50 %), 5.68 (P265, 10 Hz, 50 %), 6.05 (P265, 100 Hz, 50 %), 5.83 (P265, 1 kHz, 50 %), 5.36 (P265, 10 Hz, 90 %), 5.45 (P265, 10 Hz, 75 %), 5.88 (P265, 10 Hz, 25 %), 6.27 (P265, 10 Hz, 10 %)	*E. coli* (ATCC 11229), MS2 (ATCC 15597-B1)	–	265/P265 90 % 10 Hz/ P265 75 % 10 Hz/ P265 50 % 10 Hz/ P265 25 % 10 Hz/ P265 10 % 10 Hz: 1.96/2.10/2.04/1.85/1.8-5/1.96 (*E. coli*), 265/P265 50 % 10 Hz: 14.55/14.55 (MS2)	Batch: 50 mL total volume	PBS	(Nyangaresi et al., 2019a)
275	1.5 (1 L), 1.05 (2 L), 0.81 (3 L)[a]; 3 L: 1.30, and 6 L/h: 1.55 (1 L), 1.44 (2 L), 1.30 (3 L) [b]	*Pseudomonas aeruginosa* PA14	–	0.55 [a]; 3 L: 146.7 (3 L/h), 130.4 (6 L/h), 49.42 (15 L/h)[b]	Static mode in a cylindrical reservoir (1,2,3*L*) and depth 57, 113 and 170 mm respectively [a]; and flow-through mode in a quartz pipe of 0.207 L at 3, 6 and 15 L/h for 3 L; and 6 L/h for 1, 2 and 3 L [b]	Fresh water	(Moreno and Sun, 2008)
265, 280	–	*Bacillus subtilis* (ATCC 6633)	0.024 (265), 0.017 (280), 0.046 (280 + Cl_2 4 mg/L), 0.035 (280 + Cl_2)	40.3 (265), 59.5 (280)	Batch, 5 mL total volume, 10 mm depth	PBS	(Casado et al., 2019)
285	–	*Methylobacterium* sp.	0.012	76.88 (15 L/h), 82.05 (30 L/h), 60 (60 L/h)	Flow through mode, flow rate of 60, 30, 15	Tap water	(Wang et al., 2012b)
265, 280, 300	9.9 (265, 280), 10.1 (300)	*Pseudomonas aeruginosa*, *Legionella pneumophila*, *E. coli* IFO 3301, *Bacillus subtilis* (ATCC 6633), Qβ (ATCC 15597 B1)	0.45 (*P. aeruginosa*), 0.66 (*L. pneumophila*), 0.81 (*E. coli*), 0.085 (Qβ), 0.099 (*B. subtilis*) (LP UV); 0.77 (*P. aeruginosa*), 0.86 (*L. pneumophila*), 0.81 (*E. coli*), 0.098 (Qβ), 0.174 (*B. subtilis*) (265); 0.51 (*P. aeruginosa*), 0.45 (*L. pneumophila*), 0.56 (*E. coli*), 0.056 (Qβ), 0.104 (*B. subtilis*) (280); 0.059 (*P. aeruginosa*), 0.048 (*L. pneumophila*), 0.063 (*E. coli*), 0.006 (Qβ), 0.005 (*B. subtilis*) (300)	2.22 (*P. aeruginosa*),1.51 (*L. pneumophila*), 1.23 (*E. coli*), 11.76 (Qβ), 10.10 (*B. subtilis*) (LP UV); 1.33 (*P. aeruginosa*), 1.16 (*L. pneumophila*), 1.23 (*E. coli*), 10.20 (Qβ), 5.74 (*B. subtilis*) (265); 1.96 (*P. aeruginosa*), 2.22 (*L. pneumophila*), 1.78 (*E. coli*), 17.86 (Qβ), 9.61 (*B. subtilis*) (280)	Batch, 5 mL total volume, 7.1 mm depth	PBS	(Yan et al., 2018)
LP UV, 255, 265, 285	–	MS2	–	13.3 (255), 16.67 (265), 33.3 (285)	–	–	(Oguma et al., 2019)
385	900 and 1200	*E. coli* ATCC 25922	–	8100 (900 W/m^2) and 7200 (1200 W/m^2)	Cylindrical tank of 1 L (67 mm diameter x 300 mm depth), 240 L/h, total volume 10 L	Hydroponic nutrient solution (Amino(*OAT*) N° 1 and 2	(Keshavarzfathy and Taghipour, 2019a)
267 ± 12, 275 ± 10.5, 310 ± 8.9, 267 + 275,	3.8	*E. coli* CGMCC 1.3373	0.420 (267), 0.292 (275), 0.038 (310), 0.391 (267 + 275),	2.93 (267), 3.36 (267 + 275), 4.09 (275), 26.31 (310), 4.93	Batch, 15 mL total volume, 6 mm depth	Saline solution	(Bertagna Silva et al., 2021)

267 + 310, 275 + 310			0.203 (267 + 310), 0.149 (275 + 310)	(267 + 310), 6.71 (275 + 310)			
265 ± 11.5	0.742	Biofilm-bound *Pseudomonas aeruginosa*	–	6.2	Flow through mode, flow rate of 0.6 L/h, 14.4 L	100 mg/L TSB	(Keshavarzfathy and Taghipour, 2019b)
276 ± 10.7 (batch); 285 ± 13.5 (continuous)	3 (batch)	Total coliforms, *E. coli*, MS2 (ATCC 15597-B1)	Batch: 0.052 (MS2)	Batch: 19.23 (MS2); Continuous: 18.75 (0.6 L/h) and 18.38 (3 L/h) (MS2); 15.42 (0.6 L/h) and 10.62 (3 L/h) (Total coliforms and *E. coli*)	Batch, 5 mL, 6 mm depth; Flow through mode, flow rate of 0.6 and 3 L/h (0.686 L working volume)	Wastewater of 17.7 mg/L (COD), 3.0 mg/L (TSS), 3.9 NTU (turbidity), and 70.4 (UVT, %, 285 nm)	(Grandusky et al., 2011)
285 ± 13.5	–	MS2	–	–	Flow through mode, flow rate of 30 L/h	Tap water	(Lawal et al., 2018)
275	48.7 (245 mA), 57.6 (350 mA), 85.7 (527 mA)	MS2	Batch: 0.171 (245 mA), 0.156 (350 mA), 0.134 (527 mA)	Batch: 5 (245 mA), 5.83 (350 mA), 6.67 (527 mA)	Batch, 3.15 L; Flow through at a flow rate of 2.5×10^5 L/h	Wastewater (Turbidity: 0.09 NTU, UVT275: 97 %)	(Kojima et al., n.d.)
265, 280, 300 ± 10	–	*P. aeruginosa* (ATCC 10145), *L. pneumophila* (ATCC 33152), *E. coli* K12 IFO 3301, *Vibrio parahaemolyticus* (NBRC 12711), *B. subtilis* (ATCC 6633), Feline calcivirus (FCV) (ATCC VR-782), Qβ (ATCC 23631-B1), and MS2 (ATCC 15597-B1)	265/280: 1.039 /0.458 (*L. pneumophila*); 0.774/0.582 (*P. aeruginosa*); 0.359/0.281 (*V. parahaemolyticus*); 0.878/0.562 (*E. coli*); 0.197/0.112 (*B. subtilis*); 0.113/0.101 (FCV); 0.091/0.052 (Qβ); 0.034/0.033 (MS2)	265/280/300: 1.06 /2.2/ 21.17 (*L. pneumophila*); 1.7/2.0/23.5 (*P. aeruginosa*); 2.83/3.93/57.4 (*V. parahaemolyticus*); 1.63/2.43/23.7 (*E. coli*); 7.2/12.1/364.77 (*B. subtilis*); 8.17/9.63/144.87 (FCV); 10.3/18.0/169.9 (Qβ); 25.37/30.5/371.37 (MS2)	Batch, 5 mL total volume, 7.1 mm depth	PBS	(Wang et al., 2021)
280	–	*E. coli* K12 IFO 3301	0.43 ± 0.05	3.67	Batch, 10 mm depth	PBS	(Feng-Tie and Huang, 2011)
255, 265, 285 (UVB), 265 (33 %) + 285 (67 %), 265–285, 285–265	0.45–5.68	*E. coli K12, P. aeruginosa*, MS2.	LP U-V/255/265/285/26-5 + 285/265–285/2-85–265/P90% 265/P90% 285: 0.499/0.583/0.768/0-.403/0.371/0.475/0.-482/0.761/0.486 *(E. coli K12)*, 0.539/0.661/0.564/0-.483/0.519/0.548/0.-548/0.613/0.475 *(P. aeruginosa)*, 0.062/0.079/0.065/0-.038/0.049/0.053/0.-050/0.062/0.033 (MS2)	LP U-V/255/265/285/265 + -285/265–285/285–265/-P90% 265/P90% 285: 2.0/1.72/1.3/2.48/2.7/2-.1/2.07/1.31/2.06 *(E. coli* K12*)*, 1.86/1.52/1.77/2.07/1.9-2/1.82/1.82/1.63/2.1 *(P. aeruginosa)*, 16.1/12.66/15.38/26.31-/20.41/18.87/20/16.13/-30.3 (MS2)	Batch, 19 mL total volume, 9 mm depth	PBS	(Chen et al., 2017)
265, 280, 285, P285 (pulsed, P)	1.1 (285); 0.4 (265, 280)	*E. coli* CGMCC 1.3373	–	1.68 (P5%285); 2.4 (P50% 285); 3.05 (P100%285) (1000 Hz); 3.05 (285), 2.7–2.4 (10–1000 Hz); 4 (265, 280); 0.4 W/m^2: 4 (265, 280), 3.3 (P50%265, P50%280) (10 mJ/cm^2); 1.1 W/m^2: 3.3 (285), 2.22 (P50%285) (10 mJ/cm^2); 0.3 W/m^2: 4 (280), 2.86 (P5%2,801,000 Hz, High current) (10 mJ/cm^2)	Batch, 25 mL total volume	PBS	(Lee et al., 2021)

(continued on next page)

Table 2 (*continued*)

Wavelength (nm)	Fluence rate (W/m^2)	Microorganism	Log-linear kinetic constant (cm^2/mJ)	UV Dose response per log inactivation (mJ/cm^2)	Reactor	Water matrix	Ref.
265 ± 12.5, 275 ± 10.5	2.8	*E. coli* CGMCC 1.3373	–	3.93 (265, P265), 4.33 (275, P275)	Batch, 15 mL total volume, 6 mm depth	Saline solution	(Li et al., 2019)
265 ± 11, 285 ± 13, 365 ± 9, 265 + 285, 265 + 365,285 - + 365, 265–285, 285–265, 265–365, 365–265, 285–365, 365–285	–	*E. coli* (ATCC 11229) and MS2 (ATCC 15597-B1)	–	2.33 (265), 5.46 (285), 4.23 (265 + 285; 265–285; 285–265), Neglible (365–1160 mJ/cm^2); 435.3 (285 + 365), 405.3 (365/285), 470.12 (285–365); 727.6 (265 + 365), 646.77 (365–265), 776.13 (265–365) (*E. coli*); 12.12 (265), Neglible (365) (MS2)	Batch, 50 mL total volume	PBS	(Song et al., 2018)
265 ± 11, 365 ± 9, 365–265	–	*E. coli* (ATCC 11229), MS2 (ATCC 15597-B1)	1.14 (265), 1.11 (365–1700 mJ/-cm^2–265), 1.26 (365–17,000 mJ/-cm^2–265), 1.13 (365–52,000 mJ/-cm^2–265)	3.36 (265) (*E. coli*); 12.12 (265) (MS2)	Batch, 50 mL total volume	PBS	(Sommer et al., 1998)
265 ± 12.3, 285 ± 13.5, 265 + 285	1.9 (265), 4.4 (285); 1.8 (265), 4.1 (285)	*E. coli*, MS2 (ATCC 15597-B1)	265/285: 0.40/0.14 (*E. coli*); 0.037/0.014 (MS2)	265/285/265 + 285: 3.07/7.14/3.07 (*E. coli*), 27.02/71.42/31.11 (MS2)	Batch, 0.1 and 0.5 mL (96- and 24-multiwell plate)	PBS	(Rattanakul and Oguma, 2018)
280 ± 5	37.5	SARS-CoV-2	–	12.09	Batch	PBS	(Moreno et al., 2019)
280	4.34	*Listeria monocytogenes* (ATCC 15313, ATCC 19111, and ATCC 19115) and *Salmonella Typhimurium* (DT 104, ATCC 19585, and ATCC 43971)	10 mJ/cm^2: 0/40/120 NTU: 0.78/0.44/0.25 (*S. typhimurium*); 0.69/0.33/0.24 (*L. monocytogenes*)	10 mJ/cm^2: 0/40/120 NTU):1.54/2.25/4.85 (*S. typhimurium*); 1.44/5.95/15.87 (*L. monocytogenes*); 25 mJ/cm^2: 3.85/3.87/3.88 (*S. typhimurium*); 3.61/3.62/4.13 (*L. monocytogenes)*	Batch, 250 mL total volume	Distilled water (0 NTU), 40, 80, 120 NTU	(Gerchman et al., 2020)
260, 270, 280, 290, 310, 364, 258.5 + 260 + 270	24	Influenza A virus (IAV) H1N1	–	–	Batch, 0.3 mL total volume, 10 mm depth	PBS	(Würtele et al., 2011)
255, 265, 285	0.18 (255), 1.25 (265), 1.57 (285)	*E. coli* (ATCC 15597) and bacteriophage P22 (ATCC 19585-B1)	255/265/285: 0.178/0.150/0.109 (P22); 0.294/0.270/0.152 (*E. coli*)	255/265/285: 5.63/6.68/9.2 (P22); 5.1/5.55/9.9 (*E. coli*)	Batch, 2 mm depth	PBS	(Jarvis et al., 2019)
268 ± 12.5, 275 ± 10.5	3.8	*Bacillus cereus* (TRB-3) and *B. pumilus* (TRB-5) tetracycline resistant bacteria	–	268/275: 2.84/2.84 (TRB-3); 4.04/5.39 (TRB-5)	Batch, 15 mL total volume, 10 mm depth	PBS	(Kim et al., 2017)
255 ± 11.1, 280 ± 9.9, 255 + 280, 255 + 280 + 405, 280 + 365 + 405, 255 + 280 + 365 ± 14.9 + 405 ± 11.5	0.17 (255), 0.19 (280), 0.04 (365), 0.77 (405)	*E. coli*	–	5.88 (255), 4.28 (280), 8.76 (255 + 280)	Batch, 20 mL total volume	Treated wastewater: 10 NTU, 35.4 mg/L TOC, 14 mg/L TSS	(Hull and Linden, 2018)
265	–	MS2 (ATCC 15597 B1) and adenovirus 5 (ATCC VRS)	–	60 L/h (γ): 24; (α): 37.2 (β): 39.16 (MS2); (γ): 46.5 (Adenovirus 5). 60 L/h and (γ): Cross irradiation, UVC LED position at B or	Flow through reactor: parallel (P) and cross (C)-irradiation: UV parallel and perpendicular to the	PBS	(Oguma et al., 2016)

				C: 19.22–17.97; Parallel (*), UVC LED position at A, B or C: 16.9–14.88 (MS2)	water flow respectively. 3 modes of UV LED operation in parallel flow: (α: co-current), (β: counter-current), γ (α + β). 10 L total volume. 45, 60 and 120 L/h		
280	24 chips, Ro: 23 mm, 10 mW: 2.82 L/h:16.3; 3.6 L/h: 15.5	*E. coli* (IFO 3301)	24 chips, Ro: 23 mm, 10 mW: 0.18	24 chips, Ro: 23 mm, 10 mW: 6.35 (2.82 L/h) and 6.37 (3.6 L/h)	Flow through reactor: 2.4 and 3.6 L/h	PBS	(Yu, 2014)
265 ± 12.3, 275 ± 20, 285 ± 13.5, 295 ± 15	High/Low: 1.1/0.012–69 s/6670 s (265), 4.0/0.048–26 s/2085s (275), 3.2/0.044–18 s/1085s (285), 5.5/0.086–19 s/1300s (295)	*E. coli* MG1655	–	1.75/1.75–69 s/6670 s (265), 4.63/2.16–26 s/2085s (275), 10.53/0.91–18 s/1085s (285), 55.56/2.29–19 s/1300s (295)	Batch: 30 mL total volume, 22 mm depth	PBS	(Xiong et al., 2020)

a and b superscripts refer to the wavelength or combination of wavelengths used in each paper to facilitate the identification of the data in the subsequent columns (Fluence rate, UV Dose response per log inactivation and Log-linear kinetic constant) with their corresponding wavelengths.

sources, mainly due to their significantly smaller size, radiative pattern or photon fluence. These differences open a new universe of design possibilities for photochemical reactors for water treatment that are worth to explore.

Wang et al. (2021) highlighted the importance of achieving a uniform light distribution in the reactor. They studied three different UV LED modules of 12, 16, and 24 chips of 280 nm UV light. The UV module with 24 LED had the highest irradiance uniformity in the reactor; meanwhile, the UV module of either 12 or 16 LED led to non-uniform irradiance distributions, resulting in significant darker areas in the reactor. Similar findings were reported by other groups (Martín-Sómer et al., 2017). Wang et al. also evaluated the influence of the external radius (Ro) in an annular configuration of the reactor (19 to 27 mm) on the irradiance. They observed that values of Ro larger than 23 mm gave rise to a decrease in irradiance due to the attenuation of the UV transmittance (Wang et al., 2021). After optimising these conditions, they successfully inactivated 4 orders of magnitude of viable concentrations of *E. coli* at a flow rate of 2.82 L/h and a UV dose of 25.4 mJ/cm^2 (6.35 mJ/cm^2 per $\log_{10}$). This value can be compared with other UV fluences for 1 $\log_{10}$ inactivation obtained for 275–280 nm UV LED in batch conditions reported by other groups corresponding to 4.28 (Silva et al., 2020), 4.33 (Nyangaresi et al., 2019a), 4.09 (Nyangaresi et al., 2018), 3.67 (Yu Jeco et al., 2019), 2.43 (Oguma et al., 2019), and 1.78 (Rattanakul and Oguma, 2018) mJ/cm^2. Keshavarzfathy et al. (2021) also evaluated different radiation patterns for different 265 nm UV LED arrangements, three irradiation modes, and flow rates of 45, 60, and 120 L/h to improve the design efficiency, aiming to deliver high UV doses. For a flow rate of 60 L/h, the best UV LED arrangement led to a UV dose of 14.88–16.9 mJ/cm2 for 1 $\log_{10}$ reduction of MS2 phage compared to other reported values of 5–6.67 (Jarvis et al., 2019) and 18.38 (Nguyen et al., 2019) mJ/cm^2 for flow reactors and 25.37 (Oguma et al., 2019), 15.2 (Beck et al., n.d.), and 14.55 (Song et al., 2018) mJ/cm^2 for batch operation.

Despite the advantages of LED as a radiation source, if the light distribution is not optimised, the lighting systems are less effective than the traditional ones (Martín-Sómer et al., 2017). Fig. 3 shows the light distribution using a mercury fluorescent lamp (Hg-FL), an 8-LED system and a 40-LED system depending on the position of the lamp. The Hg-FL showed a very homogeneous distribution of the light, whereas the 8-LED system pattern is very heterogeneous, presenting highly irradiated areas corresponding to the LED locations and other areas practically in darkness. It was necessary to incorporate a higher number of LED (40-LED) to achieve a light distribution similar to that achieved with the Hg-FL system. The influence of the light distribution was studied in experiments of the photocatalytic oxidation of methanol to formaldehyde, where an improvement in the distribution of light led to a significant increase in the overall photonic efficiency of the reactor and of the bacterial inactivation. In this case, the results carried out with *E. coli* showed that there was no clear difference when using different lighting sources (Fig. 4). The existence of a highly non-uniform radiation field with regions of the reactor with very high fluence rates seemed to enhance the efficiency of the direct bacterial inactivation when LED are used, compensating the decrease in the charge transfer efficiency of the semiconductor-based photocatalytic process. In contrast, this higher photonic efficiency was counteracted by the improved bacterial inactivation achieved when the suspensions were subjected to a locally high UV fluence rate. A LED system was more efficient than traditional lamps with TiO_2 as a photocatalyst if the same UV dose was applied for a shorter period but with higher intensity, leading to high *E. coli* inactivation rates (Martín-Sómer et al., 2017). In any case, in both oxidation of chemicals and bacterial inactivation, the best option in terms of energy consumption was that with the highest number of LED due to the improvement in the light homogeneity and energy efficiency when they operated at lower electrical current intensities, considering an annular reactor configuration.

Therefore, progress is still needed regarding the optimisation of the radiation pattern and array design to ensure uniform and high UV dose delivery with optimal wavelength combinations. In this respect, it is necessary the development of precise models able to predict the radiation pattern.

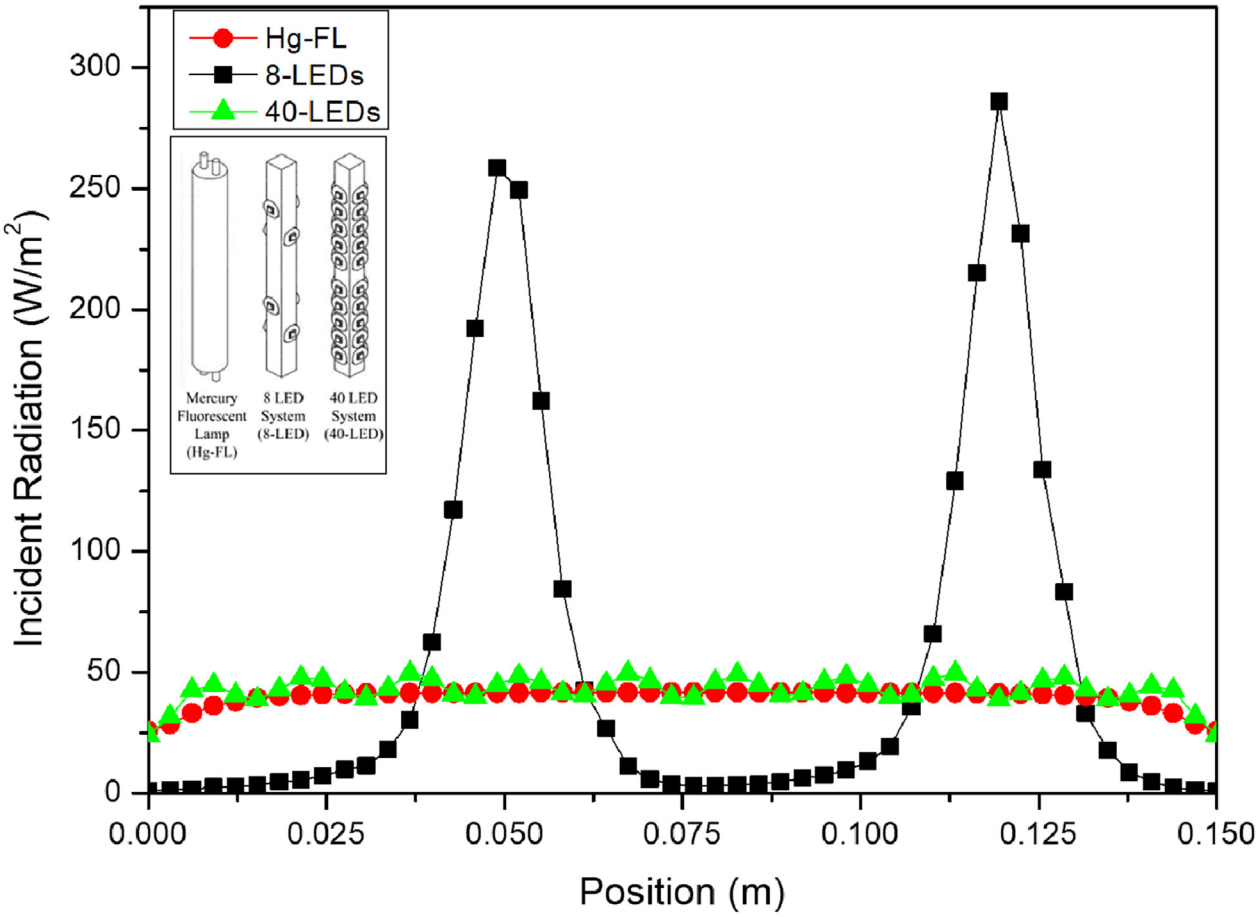

Fig. 3. Incident radiation calculated along a control line placed in the reactor area for a total incident radiation of 2.77 × 10^{-6} E/L s (Simons et al., 2014).

Some models estimated the optical output of LED by modeling the radiation from inside the LED itself, considering the optical properties of its lens (Wang et al., 2012a; Moreno and Sun, 2008; Sun et al., 2006). Some studies considered LED devices as Lambertian light sources (Grandusky et al., 2011), while others simplified the calculation by assuming a uniform light distribution in a spatial spherical cap with an angle calculated from the UV-LED viewing angle (Bowker et al., 2011; Yu, 2014). There are also studies in which the researchers obtained equations from the light distribution data reported by the manufacturers to later be able to model the light distribution in photocatalytic reactors (Simons et al., 2014; Feng-Tie and Huang, 2011). Another option that has also been studied is modeling the light distribution from the experimental measurement of the radiation profile since for water treatment applications, the radiation distribution delivered to the water solution is the important aspect without needing to know the radiation profile of the LED (Kheyrandish et al., 2018).

On the other hand, if in addition to knowing the radiative profiles, it is intended to model a certain chemical reaction, it is necessary to integrate the hydrodynamic profile of the reactor, the species transport, and the kinetics reaction into the calculation. In order to model the efficiency of a photoreactor including all these complex aspects, several models have been developed in recent years by using computational fluid dynamics (CFD) software, both commercial (García-Gil et al., 2019; Casado et al., 2019; Wang et al., 2012b; Keshavarzfathy and Taghipour, 2019a; Keshavarzfathy and Taghipour, 2019b) and open source (Moreno et al., 2019; Moreno-SanSegundo et al., 2020).

3. Conclusions

The development of UV LED devices has provided many advantages for water disinfection processes. These devices are highly efficient, have a longer lifespan, and are more adaptable to different photoreactor configurations. However, the use of LED requires a more precise understanding of photochemistry, reactor design, and the mechanism of microbial inactivation, as these parameters can substantially modify the rate of inactivation.

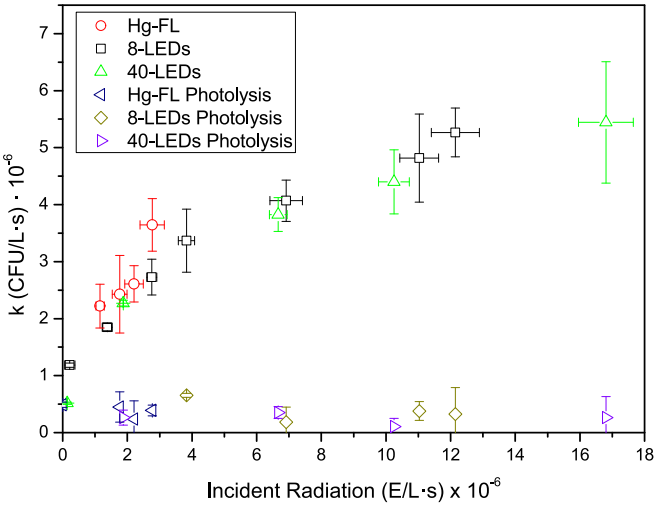

Fig. 4. Kinetic constants calculated for *E. coli* photocatalytic inactivation versus incident irradiation with the different light sources (Simons et al., 2014).

UV LED devices also allow for the selection of specific emissions wavelengths, which can be used to target specific microbial targets or to create synergistic inactivation processes. UVC LED devices, which emit at 260–265 nm, have a higher germicidal effect compared to those that emit at 280 nm. However, 280 nm radiation can also repress photoreactivation and dark repair, which may be linked to protein damage and structural damage to some enzymes involved in DNA repair. The availability of different discrete wavelengths also allows for a balance between the electrical energy efficiency of the emitter and the photochemical efficiency of the inactivation process.

UV LED sources do not require a warm-up time, which allows them to operate efficiently by pulses and enables the development of time-variable complex emission sequences. It has not been demonstrated that pulsed radiation significantly affects the efficiency of the UVC disinfection process, but it helps to improve the thermal management of the system, extending the lifetime of the low energy-efficient light sources.

The possibility of synergistic effects in microbial inactivation with UV LED combinations is still being debated, with some studies reporting no synergies and others reporting higher performance with UVA + UVC combinations for virus inactivation. The ability to fine-tune radiation intensity with UV LED allows for control of the fluence rate in real-time, which can lead to higher log inactivation at higher fluence rates and shorter exposure times. This provides a huge potential for control strategies that adapt the delivered energy to the instantaneous characteristics of the water being treated.

From the reactor design perspective, UV LED sources offer flexibility in reactor design due to their small size and adaptability, which enable a range of novel configurations and continuous treatment capacities. However, accurate simulation of the radiant field in LED reactors is crucial due to the inherently inhomogeneous distribution of the emitted light. Knowledge of the radiation pattern and array inside the photoreactors is necessary to guarantee efficient water disinfection, and precise models are needed for reactor optimisation based on the specific radiation patterns. This is especially important in photoreactors with short contact times based on the use of high-intensity light sources.

With respect to energy consumption, the optimal selection of UV LED technology for water disinfection requires balancing the quantum efficiency of the process and the electricity-to-photon conversion. UV LED of 260 nm achieves the highest bacterial inactivation but has low wall plug efficiency, while UV LED of 280 nm has a lower quantum efficiency but higher electricity conversion efficiency. A combination of a higher number of LED lamps operating at low electrical current intensities would be desirable to minimise energy consumption and heat-sinking. It is expected that the UVC LED industry will develop similar to visible and UVA LED, reaching wall plug efficiency values above 35 %, making UVC LED technology competitive for water disinfection at a large scale in the future.

CRediT authorship contribution statement

Miguel Martín-Sómer: Conceptualization, Investigation, Methodology, Writing – original draft. **Cristina Pablos:** Conceptualization, Investigation, Methodology, Writing – original draft. **Cristina Adán:** Conceptualization, Investigation, Methodology, Writing – original draft. **Rafael van Grieken:** Conceptualization, Validation, Supervision, Writing – review & editing. **Javier Marugán:** Conceptualization, Validation, Supervision, Funding acquisition, Writing – review & editing.

Data availability

Data will be made available on request.

Declaration of competing interest

The authors declare that they have no known competing financial interests or personal relationships that could have appeared to influence the work reported in this paper.

Acknowledgements

The authors gratefully acknowledge the financial support of the Spanish State Research Agency (AEI) and the Spanish Ministry of Science and Innovation through the project AQUAENAGRI (PID2021-126400OB-C32) and Comunidad de Madrid through the program REMTAVARES (P2018/EMT-4341).

References

Aparici-Espert, I., Garcia-Lainez, G., Andreu, I., Miranda, M.A., Lhiaubet-Vallet, V., 2018. Oxidatively generated lesions as internal photosensitizers for pyrimidine dimerization in DNA. ACS Chem. Biol. 13 (3), 542–547. https://doi.org/10.1021/ACSCHEMBIO.7B01097.

Baaloudj, O., Assadi, I., Nasrallah, N., El Jery, A., Khezami, L., Assadi, A.A., 2021. Simultaneous removal of antibiotics and inactivation of antibiotic-resistant bacteria by photocatalysis: a review. J. Water Process Eng. 42, 102089. https://doi.org/10.1016/J.JWPE.2021.102089.

Bertagna Silva, D., Buttiglieri, G., Babić, S., 2021. State-of-the-art and current challenges for TiO2/UV-LED photocatalytic degradation of emerging organic micropollutants. Environ. Sci. Pollut. Res. 28, 103–120. https://doi.org/10.1007/s11356-020-11125-z.

Betzalel, Y., Gerchman, Y., Cohen-Yaniv, V., Mamane, H., 2020. Multiwell plates for obtaining a rapid microbial dose-response curve in UV-LED systems. J. Photochem. Photobiol. B Biol. 207. https://doi.org/10.1016/j.jphotobiol.2020.111865.

Bourget, C.M., 2008. An introduction to light-emitting diodes. Hort. Sci. 43, 1944–1946. https://doi.org/10.21273/hortsci.43.7.1944.

Bowker, C., Sain, A., Shatalov, M., Ducoste, J., 2011. Microbial UV fluence-response assessment using a novel UV-LED collimated beam system. Water Res. 45, 2011–2019. https://doi.org/10.1016/j.watres.2010.12.005.

Cai, A., Deng, J., Zhu, T., Ye, C., Li, J., Zhou, S., Li, Q., Li, X., 2021. Enhanced oxidation of carbamazepine by UV-LED/persulfate and UV-LED/H2O2 processes in the presence of trace copper ions. Chem. Eng. J. 404, 127119. https://doi.org/10.1016/j.cej.2020.127119.

Casado, C., García-Gil, Á., van Grieken, R., Marugán, J., 2019. Critical role of the light spectrum on the simulation of solar photocatalytic reactors. Appl. Catal. B Environ. 252, 1–9. https://doi.org/10.1016/j.apcatb.2019.04.004.

Chen, J., Loeb, S., Kim, J.H., 2017. LED revolution: fundamentals and prospects for UV disinfection applications. Environ. Sci. Water Res. Technol. 3, 188–202. https://doi.org/10.1039/c6ew00241b.

Chevremont, A.C., Farnet, A.M., Sergent, M., Coulomb, B., Boudenne, J.L., 2012. Multivariate optimization of fecal bioindicator inactivation by coupling UV-A and UV-C LEDs. Desalination 285, 219–225. https://doi.org/10.1016/j.desal.2011.10.006.

Deng, Y., Li, Z., Tang, R., Ouyang, K., Liao, C., Fang, Y., Ding, C., Yang, L., Su, L., Gong, D., 2020. What will happen when microorganisms "meet" photocatalysts and photocatalysis? Environ. Sci.Nano 7, 702–723. https://doi.org/10.1039/C9EN01318K.

Dupuis, R.D., Krames, M.R., 2008. History, development, and applications of high-brightness visible light-emitting diodes. J. Light. Technol. 26. https://doi.org/10.1109/JLT.2008.923628.

Elgohary, E.A., Mohamed, Y.M.A., Nazer, H.A.El, Baaloudj, O., Alyami, M.S.S., Jery, A.El, Assadi, A.A., Amrane, A., 2021. A review of the use of semiconductors as catalysts in the photocatalytic inactivation of microorganisms. Catal. 11, 1498. https://doi.org/10.3390/CATAL11121498 2021, Vol. 11, Page 1498.

Feng-Tie, W.U., Huang, Q.-L., 2011. A Precise Model of LED Lighting and Its Application in Uni-form Illumination System. 7, pp. 1673–1905. https://doi.org/10.1007/s11801-011-1031-x.

Fujioka, T., Kodamatani, H., Yoshikawa, T., Inoue, D., Ikehata, K., 2020. Assessment of 265-nm UV-LED for direct photolysis and advanced oxidation of N-nitrosamines and 1,4-dioxane. Environ. Technol. Innov. 20, 101147. https://doi.org/10.1016/j.eti.2020.101147.

García-Gil, Á., Casado, C., Pablos, C., Marugán, J., 2019. Novel procedure for the numerical simulation of solar water disinfection processes in flow reactors. Chem. Eng. J. 376, 120194. https://doi.org/10.1016/j.cej.2018.10.131.

Gerchman, Y., Mamane, H., Friedman, N., Mandelboim, M., 2020. UV-LED disinfection of coronavirus: wavelength effect. J. Photochem. Photobiol. B Biol. 212, 112044. https://doi.org/10.1016/j.jphotobiol.2020.112044.

Gillespie, J.B., Maclean, M., Given, M.J., Wilson, M.P., Judd, M.D., Timoshkin, I.V., MacGregor, S.J., 2017. Efficacy of pulsed 405-nm light-emitting diodes for antimicrobial photodynamic inactivation: effects of intensity, frequency, and duty cycle. Photomed. Laser Surg. 35, 150–156. https://doi.org/10.1089/pho.2016.4179.

Grandusky, J.R., Gibb, S.R., Mendrick, M.C., Moe, C., Wraback, M., Schowalter, L.J., 2011. High output power from 260nm pseudomorphic ultraviolet light-emitting diodes with improved thermal performance. Appl. Phys. Express 4, 082101. https://doi.org/10.1143/APEX.4.082101.

Heathcote, B.J., 2011. UV-LED Overview Part 3- Diode Evolution and Manufacturing.

Hull, N.M., Linden, K.G., 2018. Synergy of MS2 disinfection by sequential exposure to tailored UV wavelengths. Water Res. 143, 292–300. https://doi.org/10.1016/j.watres.2018.06.017.

Hull, N.M., Herold, W.H., Linden, K.G., 2019. UV LED water disinfection: validation and small system demonstration study. AWWA Water Sci. 1, e1148. https://doi.org/10.1002/aws2.1148.

Hutchinson, F., Fuller, W., Mullins, L.J., 1980. Biological effects of ultraviolet radiation walter harm frontmatter more information. www.cambridge.org (accessed May 25, 2021).

Jarvis, P., Autin, O., Goslan, E.H., Hassard, F., 2019. Application of ultraviolet light-emitting diodes (UV-LED) to full-scale drinking-water disinfection. Water (Switzerland) 11. https://doi.org/10.3390/w11091894.

Keshavarzfathy, M., Taghipour, F., 2019. Computational modeling of ultraviolet light-emitting diode (UV-LED) reactor for water treatment. Water Res. 166, 115022. https://doi.org/10.1016/j.watres.2019.115022.
Keshavarzfathy, M., Taghipour, F., 2019. Radiation modeling of ultraviolet light-emitting diode (UV-LED) for water treatment. J. Photochem. Photobiol. A Chem. 377, 58–66. https://doi.org/10.1016/j.jphotochem.2019.03.030.
Keshavarzfathy, M., Hosoi, Y., Oguma, K., Taghipour, F., 2021. Experimental and computational evaluation of a flow-through UV-LED reactor for MS2 and adenovirus inactivation. Chem. Eng. J. 407, 127058. https://doi.org/10.1016/j.cej.2020.127058.
Kheyrandish, A., Taghipour, F., Mohseni, M., 2018. UV-LED radiation modeling and its applications in UV dose determination for water treatment. J. Photochem. Photobiol. A Chem. 352, 113–121. https://doi.org/10.1016/j.jphotochem.2017.10.047.
Kim, D.K., Kang, D.H., 2020. Inactivation efficacy of a sixteen UVC LED module to control foodborne pathogens on selective media and sliced deli meat and spinach surfaces. LWT 130, 109422. https://doi.org/10.1016/j.lwt.2020.109422.
Kim, D.K., Kim, S.J., Kang, D.H., 2017. Inactivation modeling of human enteric virus surrogates, MS2, Qβ, and ΦX174, in water using UVC-LEDs, a novel disinfecting system. Food Res. Int. 91, 115–123. https://doi.org/10.1016/j.foodres.2016.11.042.
Kim, S.S., Shin, M., Kang, J.W., Kim, D.K., Kang, D.H., 2020. Application of the 222 nm krypton-chlorine excilamp and 280 nm UVC light-emitting diode for the inactivation of Listeria monocytogenes and Salmonella typhimurium in water with various turbidities. LWT 117, 108458. https://doi.org/10.1016/j.lwt.2019.108458.
Lamar, D.G., 2020. Latest developments in LED drivers. Electronics 9, 619. https://doi.org/10.3390/electronics9040619.
Lawal, O., Cosman, J., Pagan, J., 2018. UV-C LED devices and systems: current and future state. 20. IUVA News , pp. 22–28 (accessed May 25, 2021) http://iuvanews.com/stories/pdf/IUVA_2018_Quarter1_Lawal-article_hyperlinks.pdf.
Le, T.T.T., Tran, D.T., Danh, T.H., 2021. Remarkable enhancement of visible light driven photocatalytic performance of TiO2 by simultaneously doping with C, N, and S. Chem. Phys. 545, 111144. https://doi.org/10.1016/j.chemphys.2021.111144.
Lee, H., Jin, Y., Hong, S., 2018. Understanding possible underlying mechanism in declining germicidal efficiency of UV-LED reactor. J. Photochem. Photobiol. B Biol. 185, 136–142. https://doi.org/10.1016/j.jphotobiol.2018.06.001.
Lee, H.K., Jang, H., Kim, N., Joo, J.B., 2021. Cu-doped TiO2 hollow nanostructures for the enhanced photocatalysis under visible light conditions. J. Ind. Eng. Chem. https://doi.org/10.1016/j.jiec.2021.04.045.
Levchuk, I., Rueda-Márquez, J.J., Suihkonen, S., Manzano, M.A., Sillanpää, M., 2015. Application of UVA-LED based photocatalysis for plywood mill wastewater treatment. Sep. Purif. Technol. 143, 1–5. https://doi.org/10.1016/j.seppur.2015.01.007.
Li, G.-Q.Q., Wang, W.-L.L., Huo, Z.-Y.Y., Lu, Y., Hu, H.-Y.Y., 2017. Comparison of UV-LED and low pressure UV for water disinfection: photoreactivation and dark repair of Escherichia coli. Water Res. 126, 134–143. https://doi.org/10.1016/j.watres.2017.09.030.
Li, X., Cai, M., Wang, L., Niu, F., Yang, D., Zhang, G., 2019. Evaluation survey of microbial disinfection methods in UV-LED water treatment systems. Sci. Total Environ. 659, 1415–1427. https://doi.org/10.1016/j.scitotenv.2018.12.344.
Liu, X., Pan, L., Lv, T., Sun, Z., 2014. CdS sensitized TiO2 film for photocatalytic reduction of Cr(VI) by microwave-assisted chemical bath deposition method. J. Alloys Compd. 583, 390–395. https://doi.org/10.1016/j.jallcom.2013.08.193.
M. Kojima K. Mawatari T. Emoto R. Nishisaka-Nonaka T. Kim N. Bui T. Shimohata T. Uebanso M. Akutagawa Y. Kinouchi T. Wada M. Okamoto H. Ito K. Tojo T. Daidoji T. Nakaya A. Takahashi Microorganisms irradiation by a combination of different peak-wavelength ultraviolet-light emitting diodes enhances the inactivation of influenza s viruses, (n.d.). doi:10.3390/microorganisms8071014.
Martino, V., Ochsner, K., Peters, P., Zitomer, D.H., Mayer, B.K., 2020. Virus and bacteria inactivation using ultraviolet light-emitting diodes. Environ. Eng. Sci. 38, 458–468. https://doi.org/10.1089/ees.2020.0092.
Martín-Sómer, M., Pablos, C., van Grieken, R., Marugán, J., 2017. Influence of light distribution on the performance of photocatalytic reactors: LED vs mercury lamps. Appl. Catal. B Environ. 215, 1–7. https://doi.org/10.1016/j.apcatb.2017.05.048.
Martín-Sómer, M., Vega, B., Pablos, C., van Grieken, R., Marugán, J., 2018. Wavelength dependence of the efficiency of photocatalytic processes for water treatment. Appl. Catal. B Environ. 221, 258–265. https://doi.org/10.1016/J.APCATB.2017.09.032.
Martín-Sómer, M., Benz, D., van Ommen, J.R., Marugán, J., 2020. Multitarget evaluation of the photocatalytic activity of P25-SiO2 prepared by atomic layer deposition. Catalysts 10, 450. https://doi.org/10.3390/catal10040450.
Moreno, I., Sun, C.-C., 2008. Modeling the radiation pattern of LEDs. Opt. Express 16, 1808. https://doi.org/10.1364/oe.16.001808.
Moreno, J., Casado, C., Marugán, J., 2019. Improved discrete ordinate method for accurate simulation radiation transport using solar and LED light sources. Chem. Eng. Sci. 205, 151–164 (accessed July 11, 2019) https://www.sciencedirect.com/science/article/pii/S000925091930404X.
Moreno-SanSegundo, J., Casado, C., Marugán, J., 2020. Enhanced numerical simulation of photocatalytic reactors with an improved solver for the radiative transfer equation. Chem. Eng. J. 388, 124183. https://doi.org/10.1016/j.cej.2020.124183.
Natarajan, T.S., Thomas, M., Natarajan, K., Bajaj, H.C., Tayade, R.J., 2011. Study on UV-LED/TiO2 process for degradation of Rhodamine B dye. Chem. Eng. J. 169, 126–134. https://doi.org/10.1016/j.cej.2011.02.066.
Nguyen, T.M.H., Suwan, P., Koottatep, T., Beck, S.E., 2019. Application of a novel, continuous-feeding ultraviolet light emitting diode (UV-LED) system to disinfect domestic wastewater for discharge or agricultural reuse. Water Res. 153, 53–62. https://doi.org/10.1016/j.watres.2019.01.006.
Nyangaresi, P.O., Qin, Y., Chen, G., Zhang, B., Lu, Y., Shen, L., 2018. Effects of single and combined UV-LEDs on inactivation and subsequent reactivation of E. coli in water disinfection. Water Res. 147, 331–341. https://doi.org/10.1016/j.watres.2018.10.014.
Nyangaresi, P.O., Qin, Y., Chen, G., Zhang, B., Lu, Y., Shen, L., 2019. Comparison of the performance of pulsed and continuous UVC-LED irradiation in the inactivation of bacteria. Water Res. 157, 218–227. https://doi.org/10.1016/j.watres.2019.03.080.
Nyangaresi, P.O., Qin, Y., Chen, G., Zhang, B., Lu, Y., Shen, L., 2019. Comparison of UV-LED photolytic and UV-LED/TiO2 photocatalytic disinfection for Escherichia coli in water. Catal. Today 335, 200–207. https://doi.org/10.1016/j.cattod.2018.11.015.
Oguma, K., Rattanakul, S., Bolton, J.R., 2016. Application of UV light–emitting diodes to adenovirus in water. J. Environ. Eng. 142, 04015082. https://doi.org/10.1061/(asce)ee.1943-7870.0001061.
Oguma, K., Rattanakul, S., Masaike, M., 2019. Inactivation of health-related microorganisms in water using UV light-emitting diodes. Water Sci. Technol.Water Supply 19, 1507–1514. https://doi.org/10.2166/ws.2019.022.
Ohl, R.S., 1946. Alternating Current Rectifier.
Oppezzo, O.J., Pizarro, R.A., 2001. Sublethal effects of ultraviolet a radiation on Enterobacter cloacae. J. Photochem. Photobiol. B Biol. 62, 158–165. https://doi.org/10.1016/S1011-1344(01)00180-4.
Pousty, D., Hofmann, R., Gerchman, Y., Mamane, H., 2021. Wavelength-dependent time–dose reciprocity and stress mechanism for UV-LED disinfection of Escherichia coli. J. Photochem. Photobiol. B Biol. 217, 112129. https://doi.org/10.1016/j.jphotobiol.2021.112129.
Rattanakul, S., Oguma, K., 2018. Inactivation kinetics and efficiencies of UV-LEDs against Pseudomonas aeruginosa, Legionella pneumophila, and surrogate microorganisms. Water Res. 130, 31–37. https://doi.org/10.1016/j.watres.2017.11.047.
Ray, S.K., Dhakal, D., Regmi, C., Yamaguchui, T., Lee, S.W., 2018. Inactivation of Staphylococcus aureus in visible light by morphology tuned α-NiMoO4. J. Photochem. Photobiol. A Chem. 350, 59–68. https://doi.org/10.1016/J.JPHOTOCHEM.2017.09.042.
Rediker, R.H., 1987. Research at Lincoln Laboratory leading up to the development of the injection laser in 1962. IEEE J. Quantum Electron. 23, 692–695. https://doi.org/10.1109/JQE.1987.1073430.
Repo, E., Rengaraj, S., Pulkka, S., Castangnoli, E., Suihkonen, S., Sopanen, M., Sillanpää, M., 2013. Photocatalytic degradation of dyes by CdS microspheres under near UV and blue LED radiation. Sep. Purif. Technol. 120, 206–214. https://doi.org/10.1016/j.seppur.2013.10.008.
Rodríguez-González, V., Obregón, S., Patrón-Soberano, O.A., Terashima, C., Fujishima, A., 2020. An approach to the photocatalytic mechanism in the TiO2-nanomaterials microorganism interface for the control of infectious processes. Appl. Catal. B Environ. 270, 118853. https://doi.org/10.1016/J.APCATB.2020.118853.
Round, H.J., 1991. A note on carborundum. Semicond. Devices Pioneer. Pap, p. 879 https://doi.org/10.1142/9789814503464_0116.
S.E. Beck, H. Ryu, L.A. Boczek, J.L. Cashdollar, K.M. Jeanis, J.S. Rosenblum, O.R. Lawal, K.G. Linden, Evaluating UV-C LED disinfection performance and investigating potential dual-wavelength synergy, Water Res. 109 (n.d.) 207–216. doi:10.1016/j.watres.2016.11.024.
Saravanan, A., Kumar, P.S., Jeevanantham, S., Karishma, S., Kiruthika, A.R., 2021. Photocatalytic disinfection of micro-organisms: mechanisms and applications. Environ. Technol. Innov. 24, 101909. https://doi.org/10.1016/J.ETI.2021.101909.
Shen, L., Griffith, T.M., Nyangaresi, P.O., Qin, Y., Pang, X., Chen, G., Li, M., Lu, Y., Zhang, B., 2020. Efficacy of UVC-LED in water disinfection on Bacillus species with consideration of antibiotic resistance issue. J. Hazard. Mater. 386, 121968. https://doi.org/10.1016/j.jhazmat.2019.121968.
Sholtes, K., Linden, K.G., 2019. Pulsed and continuous light UV LED: microbial inactivation, electrical, and time efficiency. Water Res. 165, 114965. https://doi.org/10.1016/j.watres.2019.114965.
Sholtes, K.A., Lowe, K., Walters, G.W., Sobsey, M.D., Linden, K.G., Casanova, L.M., 2016. Comparison of ultraviolet light-emitting diodes and low-pressure mercury-arc lamps for disinfection of water. Environ. Technol. (UK) 37, 2183–2188. https://doi.org/10.1080/09593330.2016.1144798.
Silva, N.B., Leonel, L.P., Tonetti, A.L., 2020. UV-LED for safe effluent reuse in agriculture. Water Air Soil Pollut. 231, 1–10. https://doi.org/10.1007/s11270-020-04742-4.
Simons, R., Gabbai, U.E., Moram, M.A., 2014. Optical fluence modelling for ultraviolet light emitting diode-based water treatment systems. Water Res. 66, 338–349. https://doi.org/10.1016/j.watres.2014.08.031.
Sommer, R., Haider, T., Cabaj, A., Pribil, W., Lhotsky, M., 1998. Time Dose Reciprocity in UV Disinfection of Water. https://doi.org/10.1016/S0273-1223(98)00816-6 No longer published by Elsevier.
Song, K., Taghipour, F., Mohseni, M., 2018. Microorganisms inactivation by continuous and pulsed irradiation of ultraviolet light-emitting diodes (UV-LEDs). Chem. Eng. J. 343, 362–370. https://doi.org/10.1016/j.cej.2018.03.020.
Song, K., Taghipour, F., Mohseni, M., 2019. Microorganisms inactivation by wavelength combinations of ultraviolet light-emitting diodes (UV-LEDs). Sci. Total Environ. 665, 1103–1110. https://doi.org/10.1016/j.scitotenv.2019.02.041.
Song, K., Mohseni, M., Taghipour, F., 2019. Mechanisms investigation on bacterial inactivation through combinations of UV wavelengths. Water Res. 163, 114875. https://doi.org/10.1016/j.watres.2019.114875.
Sun, C.-C., Lee, T.-X., Ma, S.-H., Lee, Y.-L., Huang, S.-M., 2006. Precise optical modeling for LED lighting verified by cross correlation in the midfield region. Opt. Lett. 31, 2193. https://doi.org/10.1364/ol.31.002193.
Takahashi, K., Matsubayashi, M., Ohashi, Y., Naohara, J., Urakami, I., Sasai, K., Kido, Y., Kaneko, A., Teramoto, I., 2020. Efficacy of ultraviolet light-emitting diodes (UV-LED) at four different peak wavelengths against Cryptosporidium parvum oocysts by inactivation assay using immunodeficient mice. Parasitol. Int. 77, 102108. https://doi.org/10.1016/j.parint.2020.102108.
Thatcher, C.H., Adams, B.R., 2021. Impact of surface reflection on microbial inactivation in a UV LED treatment duct. Chem. Eng. Sci. 230, 116204. https://doi.org/10.1016/j.ces.2020.116204.

Tokode, O., Prabhu, R., Lawton, L.A., Robertson, P.K.J., 2016. Controlled periodic illumination in semiconductor photocatalysis. J. Photochem. Photobiol. A Chem. 319–320, 96–106. https://doi.org/10.1016/j.jphotochem.2015.12.002.

Wang, C.P., Chang, C.S., Lin, W.C., 2021. Efficiency improvement of a flow-through water disinfection reactor using UV-C light emitting diodes. J. Water Process Eng. 40, 101819. https://doi.org/10.1016/j.jwpe.2020.101819.

Wang, G., Wang, L., Li, F., Zhang, G., 2012. Collimating lens for light-emitting-diode light source based on non-imaging optics. Appl. Opt. 51, 1654–1659. https://doi.org/10.1364/AO.51.001654.

Wang, Z., Liu, J., Dai, Y., Dong, W., Zhang, S., Chen, J., 2012. CFD modeling of a UV-LED photocatalytic odor abatement process in a continuous reactor. J. Hazard. Mater. 215–216, 25–31. https://doi.org/10.1016/j.jhazmat.2012.02.021.

Weisbuch, C., 2020. Review: on the search for efficient solid state light emitters: past, present, future. ECS J. Solid State Sci. Technol. 9, 016022. https://doi.org/10.1149/2.0392001jss.

Würtele, M.A., Kolbe, T., Lipsz, M., Külberg, A., Weyers, M., Kneissl, M., Jekel, M., 2011. Application of GaN-based ultraviolet-C light emitting diodes - UV LEDs - for water disinfection. Water Res. 45, 1481–1489. https://doi.org/10.1016/j.watres.2010.11.015.

Xiao, Y., Chu, X.N., He, M., Liu, X.C., Hu, J.Y., 2018. Impact of UVA pre-radiation on UVC disinfection performance: inactivation, repair and mechanism study. Water Res. 141, 279–288. https://doi.org/10.1016/j.watres.2018.05.021.

Xiong, P., Hu, J., 2013. Inactivation/reactivation of antibiotic-resistant bacteria by a novel UVA/LED/TiO2 system. Water Res. 47, 4547–4555. https://doi.org/10.1016/j.watres.2013.04.056.

Xiong, P., Hu, J., 2017. Decomposition of acetaminophen (Ace) using TiO2/UVA/LED system. Catal. Today 282, 48–56. https://doi.org/10.1016/j.cattod.2016.03.015.

Xiong, R., Lu, Z., Tang, Q., Huang, X., Ruan, H., Jiang, W., Chen, Y., Liu, Z., Kang, J., Liu, D., 2020. UV-LED/chlorine degradation of propranolol in water: degradation pathway and product toxicity. Chemosphere 248, 125957. https://doi.org/10.1016/j.chemosphere.2020.125957.

Yan, Y., Zhou, X., Lan, J., Li, Z., Zheng, T., Cao, W., Zhu, N., Liu, W., 2018. Efficient photocatalytic disinfection of Escherichia coli by N-doped TiO2 coated on coal fly ash cenospheres. J. Photochem. Photobiol. A Chem. 367, 355–364. https://doi.org/10.1016/j.jphotochem.2018.08.045.

Yin, R., Shang, C., 2020. Removal of micropollutants in drinking water using UV-LED/chlorine advanced oxidation process followed by activated carbon adsorption. Water Res. 185, 116297. https://doi.org/10.1016/j.watres.2020.116297.

Yu Jeco, B.M.F., Larroder, A.C., Oguma, K., 2019. Technosocial feasibility analysis of solar-powered UV-LED water treatment system in a remote island of Guimaras, Philippines. J. Photonics Energy 9, 1. https://doi.org/10.1117/1.jpe.9.043105.

Yu, L., 2014. Light Emitting Diode Based Photochemical Treatment of Contaminants in Aqueous Phase. University of Calgary https://doi.org/10.11575/PRISM/26762.

Zhang, Q., Wang, Y., Zhu, X., Liu, X., Li, H., 2021. 1T and 2H mixed phase MoS2 nanobelts coupled with Ti3+ self-doped TiO2 nanosheets for enhanced photocatalytic degradation of RhB under visible light. Appl. Surf. Sci. 556, 149768. https://doi.org/10.1016/j.apsusc.2021.149768.

Zheludev, N., 2007. The life and times of the LED - a 100-year history. Nat. Photonics 1, 189–192. https://doi.org/10.1038/nphoton.2007.34.

Zhou, X., Li, Z., Lan, J., Yan, Y., Zhu, N., 2017. Kinetics of inactivation and photoreactivation of Escherichia coli using ultrasound-enhanced UV-C light-emitting diodes disinfection. Ultrason. Sonochem. 35, 471–477. https://doi.org/10.1016/j.ultsonch.2016.10.028.

Zou, X.Y., Lin, Y.L., Xu, B., Cao, T.C., Tang, Y.L., Pan, Y., Gao, Z.C., Gao, N.Y., 2019. Enhanced inactivation of E. coli by pulsed UV-LED irradiation during water disinfection. Sci. Total Environ. 650, 210–215. https://doi.org/10.1016/j.scitotenv.2018.08.367.